Journal Pre-proofs

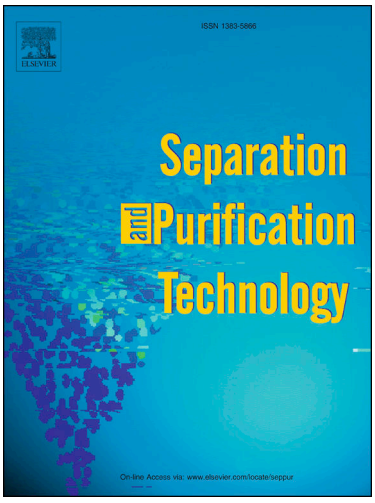

Membrane-based enrichment of omega-3 fatty acids in fish oil: Techno-economic study

M. Ongis, G. Di Marcoberardino, D. Ormerod, F. Gallucci, M. Binotti

PII: S1383-5866(24)04929-3
DOI: https://doi.org/10.1016/j.seppur.2024.131190
Reference: SEPPUR 131190

To appear in: *Separation and Purification Technology*

Received Date: 9 October 2024
Revised Date: 13 December 2024
Accepted Date: 17 December 2024

Please cite this article as: M. Ongis, G. Di Marcoberardino, D. Ormerod, F. Gallucci, M. Binotti, Membrane-based enrichment of omega-3 fatty acids in fish oil: Techno-economic study, *Separation and Purification Technology* (2024), doi: https://doi.org/10.1016/j.seppur.2024.131190

This is a PDF file of an article that has undergone enhancements after acceptance, such as the addition of a cover page and metadata, and formatting for readability, but it is not yet the definitive version of record. This version will undergo additional copyediting, typesetting and review before it is published in its final form, but we are providing this version to give early visibility of the article. Please note that, during the production process, errors may be discovered which could affect the content, and all legal disclaimers that apply to the journal pertain.

© 2024 The Author(s). Published by Elsevier B.V.

Journal Pre-proofs

Membrane-based enrichment of omega-3 fatty acids in fish oil: techno-economic study

M. Ongis[1,2,*], G. Di Marcoberardino[3], D. Ormerod[4], F. Gallucci[2] and M. Binotti[1,*]

[1]*Group of Energy Conversion Systems, Department of Energy, Politecnico di Milano, via Lambruschini 4a, 20156, Milano, Italy*
[2] *Inorganic Membranes and Membrane Reactors, Sustainable Process Engineering, Department of Chemical Engineering and Chemistry, Eindhoven University of Technology, PO Box 513, 5600 MB, Eindhoven, The Netherlands*
[3]*Dipartimento di Ingegneria Meccanica e Industriale, Università degli Studi di Brescia, via Branze 38, 25123, Brescia, Italy*
[4]*VITO, (Flemish Institute for Technology Reseach), Materials & Chemistry, Boeretang 200, B-2400 Mol, Belgium*

(*) michele.ongis@polimi.it; marco. binotti@polimi.it

Abstract

Concentrated ω3 fatty acids products represent an important support for their recommended intake in human diet. Several concentration routes exist nowadays, depending also on the desired enrichment level. One of the emerging solutions is the use of membranes, coupled with the enzymatic enrichment route. In this scenario, a lipase uses ethanol to selectively detach from the triglycerides short chain acids, leaving polyunsaturated fatty acids attached. Reaction mixture is then sent to a dense polymeric membrane, able to retain preferentially the enriched glycerides allowing ethyl esters to cross the membrane more easily. To assess the potential benefits of this innovative route, modelling activity is a fundamental support. In literature, several studies investigated solvent nanofiltration through membranes, although studies at process scale are still limited and this also limits the diffusion of membrane technology. In this work, both a kinetic and membrane section models are used to develop the process model of the system. A techno-economic analysis is performed to estimate the levelized cost of the enriched oil as function of the level of enrichment. Results are compared with a benchmark process based on a non-selective transesterification of the acids followed by molecular distillation. Membrane-based process is able to enrich the oil from 31.65% up to 54% (a factor 1.7), while the higher the enrichment, the more the oil input needed per unit of product, the higher the product cost. Considering as feedstock fish oil with a cost of 10 €/kg, the products cost ranges from 13 €/kg at low enrichment up to 33.2 €/kg at 1.7, outperforming the results of the benchmark solution (from 16.5 €/kg to 39.2 €/kg in the same range) and therefore assessing the potential gains in membranes' application in this process.

Keywords: Modeling; ω3 concentration; fatty acid enrichment; polymeric membrane; techno-economic

1. Introduction

ω3 are polyunsaturated fatty acids (PUFA) represent an important intake in human diet, since their consumption is related to the reduced risk of several illnesses, such as hypertriglyceridemia and ovarian cancer [1]–[3], and to the support of different brain functions [4]. ω3 supplements might represent an important support whenever their overall consumption is below recommendations [5]. In principle, even from direct extraction from specific marine sources (i.e. fish and algae, without the necessity of their concentration) it is possible to obtain oils with ω3 content about 20-40% of the total acids' moles [6].

However, there is both health and market interest in the concentration of these acids, in order to reduce the overall fatty acids intake while maintaining the recommended intake of ω3. This is translated into a technical interest, where several techniques exist, ranging from mild (about 50%) to high (about 85%) up to very high (>95%) concentrations, using both physical and chemical methods. According to [7], to concentrate any fish oil it is firstly necessary to convert the natural triglycerides (TAG) into ethyl esters (EE) or into free fatty acids (FFA). This can be done by detaching all acids using a strong based or acid catalyst, thus moving the problem of the ω3 enrichment in this form, or selectively detaching specific acids through a lipase, typically leaving bonded to the glycerol backbone the long-chain PUFA. In the former case, there exists several techniques to concentrate the ω3 fraction in EE or FFA form, such as urea precipitation, crystallization at low temperatures, supercritical fluid extraction, supercritical fluid chromatography and molecular distillation, which can separate the acids based on carbon chain length and/or saturation degree. The different methods have different operating conditions, costs and level of product enrichment, which have been extensively reviewed [6]–[8]. Among them, molecular distillation (MD) has been selected in this article as benchmark process, since it represents the most commercially diffused technique [7] for mild/high enrichment with low investment costs. It represents a high vacuum distillation technique, where physical distance between evaporation and condensation is smaller than the mean free path of the molecules [9]. As it separates components based on different volatility (different boiling points), it is able to separate acids according to the chain length but does not distinguish among different degrees of saturation [7]. This is the reason of the upper limit to the concentration, and for this reason this technique is sometimes coupled with other ones when very high concentrations are desired. Enriched products, in form of EE, can be then re-esterified to glyceride products to increase the ω3 bioavailability [10].

In the enzymatic enrichment route, on the other hand, the problem is mainly to separate the acylglycerol enriched fraction from the depleted detached (EE or FFA) acids. Also in this situation, MD represents the common route to remove the depleted light fraction [7]. In this case, all the optimization of the process depends on the development of optimized enzyme formulations. Another technique that is emerging as a potential candidate for this process is the usage of membranes. As low-cost technology, membranes can be used for the purification step to remove the depleted EE fraction while retaining the acylglycerols. Very few studies exists in literature about membranes use in EE or methyl esters separation. The possibility to use polymeric membranes for ω3 enrichment was firstly reported by Ghasemian et al. [11], and recent literature only contains two examples of membranes used for ethyl or methyl esters separation in different processes, as reported by

Eyskenis et al. [8]. So far, membranes use is limited due to limited selectivity and the high specificity of each permeation process, that makes it difficult to have accurate predictions in case of complex mixtures. However, membrane application is still increasing as more research is done, and new applications are based on glycerides separation from EEs based on molecular size or polarity. Membrane technology represents in this sector a potential profitable route worth to be investigated. In EU funded project MACBETH, a pilot plant for oil enrichment coupling enzymatic route and membrane technology has been developed and operated [12]. As oil is a highly viscous component, it should be typically diluted in a low-viscosity component that crosses easily the membrane and drags preferentially smaller components with him. Membrane process to selectively separate components as small as glycerides falls in the organic solvent nanofiltration (OSN) category.

Mathematical modelling is a fundamental support to optimize membrane performance and the process design and to favor membrane diffusion. Transport models of OSN can be divided, according to different reviews, in irreversible thermodynamics models, solution-diffusion models and pore flow models [13]–[15]. Descriptions differ in their assumptions and descriptions of the variables profiles, although they can be sometimes used equivalently as they represents complementary approaches of the problem [16]. Solution-diffusion model [17], as it is found in most of the publications on the topic, has been adopted also in this work [18]–[22]. In particular, among the different formulations that the model may have, the mathematical derivation of Peeva [23] is the one adopted in this work. According to [24], more than 90% on the publications were at membrane scale, meaning that are based on tuning the transport equation and rejections of solutes. Only, respectively, 4% and 5% were about module and process scale. At module scale, different operational modes can be used, such as batch, constant-volume semi-batch [25] and continuous steady state [24]. Process scale is on the other hand dependent on the specific process, and its poor investigation is possibly among the causes of the low diffusion on membranes in the sector.

Aim of this article is to assess the potentialities of the usage of polymeric membranes for ω3 concentration, by studying the whole process through a techno-economic assessment. The plant model is based on mathematical models of both transesterification reactor and membrane unit. Techno-economic results are compared with the benchmark technology, represented by the conventional alkali-based transesterification to EE followed by MD unit.

Journal Pre-proofs

2. Methodology

2.1 Fish oil composition

Fish oil composition in terms of fatty acids fractions is taken from [26] and is reported in Table 1. It is assumed that all acids are in triglyceride form in raw fish oil. Oil density is 930 g/L, and its molar mass is 876.115 g/mol. Molar volume therefore results 0.9421 L/mol, and it is assumed to be constant in the process and for the different oil products.

Table 1: raw fish oil composition in terms of fatty acids

Acid name	Acid index i	Acid code	Mole fraction
(-)	(-)	(-)	(%)
Myristic	1	C14:0	10.87
Palmitic	2	C16:0	20.85
Palmitoleic	3	C16:1	12.30
Stearic	4	C18:0	3.49
Oleic	5	C18:1 cis9	8.89
Octadecenoic	6	C18:1 cis11	3.67
Linoleic	7	C18:2	1.32
Linolenic	8	C18:3	0.89
Arachidic	9	C20:0	3.45
Eicosenoic	10	C20:1	0.66
Eicosapentaenoic (EPA)	11	C20:5	19.45
DPA	12	C22:5	1.94
Docosahexaenoic (DHA)	13	C22:6	12.20

From Table 1 it can be derived that the initial molar fraction of EPA and DHA combined, that represent the ω3 fatty acids of interest, is 31.65% (35.06% in mass fraction). Aim of the process design is to find the optimum between the increase in EPA and DHA concentration and their loss in the enrichment process.

2.2 Methods

To avoid issues related to volume variation (changing when density changes) and masses (the same molar enrichment can have different mass values depending on the glyceride ester form) all calculations are performed on a molar basis. The benchmark and the membrane-based processes are both designed to obtain 10 L/h of oil produced which corresponds to 10.615 mol/h of TAGs and to 31.845 mol/h of fatty acids. However, the final product is not a mixture of TAGs, but it will contain all esters form of acids bounded to ethanol and glycerol. In all simulations, it is however guaranteed that the enriched products has a content of 31.845 mol/h of fatty acids.

The methodology of the work is to compare the performance of the membrane-based process, consisting in an enzymatic transesterification followed by a separation step using polymeric membranes, and the benchmark process, based on total conversion to ethyl esters followed by molecular distillation. They are summarized in Figure 1. Process models are realized in Aspen Plus®, while customized blocks (enzymatic reactor, polymeric membrane) have been developed in Aspen Custom Modeler® and then integrated in the Aspen Plus flowsheet. Oil properties are modelled using UNIFAC Dortmund modified method.

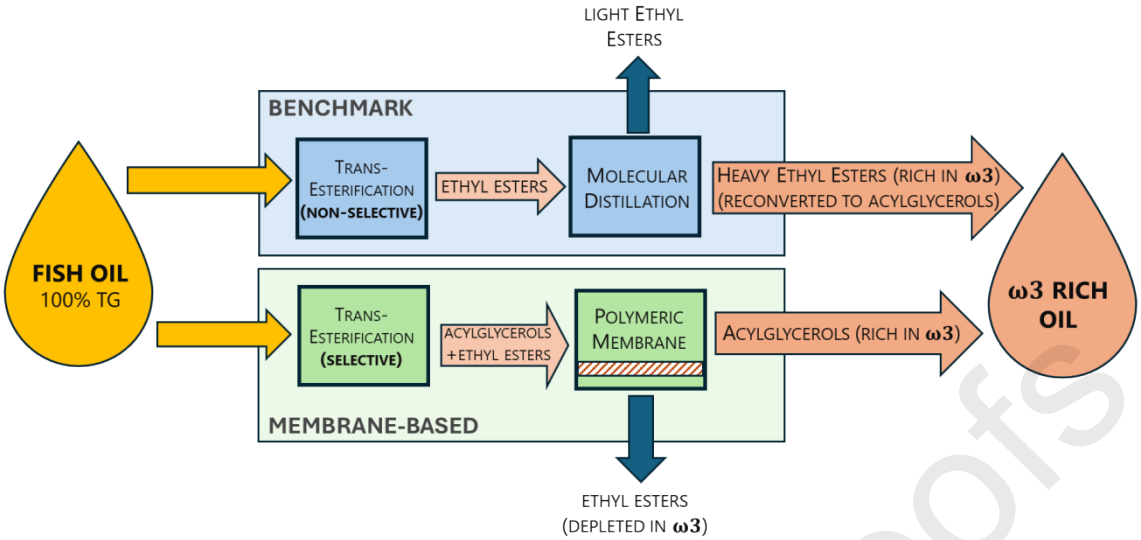

Figure 1: processes compared for fish oil concentration.

For the benchmark process, plant layout, assumptions and molecular distillation modeling is presented in section 3. Values and information are mainly taken from literature.

Membrane-based solution is presented in detail in section 4. The kinetics of the transesterification is based on an innovative formulation of a kinetic model, developed by the same authors in a previous work [26]. For the membrane section, experiments have been performed to determine the permeabilities of the different components, used in the solution-diffusion description of the flux and then integrated in the membrane module description. Description in detail is in section 4.3.

For both solutions, technical and economic Key Performance Indicators (KPIs) are calculated aiming at assessing the potentialities of the membrane-based solution.

2.3 Key performance indicators

Aim of the process is to produce an oil mixture enriched in target ω3 acids (EPA and DHA). In doing so, inevitably some of these acids will get lost in the depleted fraction of the oil. These two effects, between which there exists a trade-off, are described by two KPIs respectively: the *oil enrichment* and the *target recovery*. Oil enrichment is defined, in terms of mole fractions, as the ratio between molar fraction of EPA and DHA in final product over their molar fraction in the raw oil, which is 31.65%. It is therefore a number >1 when a certain enrichment is achieved. In mathematical terms, is defined in equation (1**)**.

Target recovery is the ratio between moles of ω3 in the final product over the total amount fed into the system in the raw oil. In other words, it represents the share of ω3 moles fed to the system that can be found in the final product, defined mathematically in equation (2**)**. Their complement-to-one represents the share of ω3 lost in the process.

$$OE = \frac{\left.\frac{\dot{n}_{EPA} + \dot{n}_{DHA}}{\dot{n}_{all\ acids}}\right|_{enriched\ oil}}{\left.\frac{\dot{n}_{EPA} + \dot{n}_{DHA}}{\dot{n}_{all\ acids}}\right|_{raw\ oil}} = \frac{x_{\omega 3, enriched\ oil}}{x_{\omega 3,\ raw\ oil}} \qquad (1)$$

$$TR = \frac{\dot{n}_{EPA} + \dot{n}_{DHA}|_{enriched\ oil}}{\dot{n}_{EPA} + \dot{n}_{DHA}|_{raw\ oil}} = 1 - \frac{\dot{n}_{EPA} + \dot{n}_{DHA}|_{depleted\ oil}}{\dot{n}_{EPA} + \dot{n}_{DHA}|_{raw\ oil}} \quad (2)$$

Together with this parameters, energy and environmental performances of the plant are assessed by an evaluation of its specific energy consumption (i.e. primary energy per kg of final product, SEC) and specific GreenHouse Gases (GHGs) emissions (i.e. equivalent CO_2 emissions per kg of final product, $E_{CO_2,eq}$). Definitions are reported in equations (3**)** and (4**)**, respectively.

$$SEC = \frac{\frac{\dot{W}}{\eta_{el,ref}} + \dot{Q}}{\dot{m}_{enriched\ oil}} \quad (3)$$

$$E_{CO_2,eq} = \frac{\dot{W} \cdot GWP_{el} + \dot{Q} \cdot GWP_{th} + \dot{m}_{raw\ oil} \cdot GWP_{raw\ oil}}{\dot{m}_{enriched\ oil}} \quad (4)$$

Where $\dot{W}$ and $\dot{Q}$ are the electric and thermal power, respectively, required by the process. Average efficiency of electricity production $\eta_{el,ref}$ is assumed 0.45 [27], global warming potential (GWP) associated to electricity is 352 g_{CO_2}/kW_{el} and for thermal power 201 g_{CO_2}/kW_{th} [28]. Relevant electrical and thermal consumptions in the two processes are related to the distillation columns, as it will be described in the next sections. Thermal duty is calculated from the column design in the process simulator, while electricity is estimated as fraction of the thermal duty. Feed pumps consumption is neglected, while extraction pumps after the distillation columns are integrated in the column consumptions. In equation (4**)** is also included a term for the emissions related to raw fish oil production. According to Global Feed Lifecycle Assessment Institute database, the footprint of fish oil is quite variable, and as an average value it results 830 $g_{CO_2}/kg_{raw\ oil}$ [29]. On the other hand, calculations made in a recent article obtained a value of 2,690 $g_{CO_2}/kg_{raw\ oil}$ [30]. Therefore, in this article, a value in between the two is used for the analysis, equal to 1,760 $g_{CO_2}/kg_{raw\ oil}$.

From the economic point of view, the aim is to determine the Levelized Cost Of Product (LCOP), where for product it is meant the enriched oil. Levelized cost is calculated according to the equation:

$$LCOP = \frac{TPC \cdot CCF + O\&M_{fix} + O\&M_{var} \cdot h_{eq}}{\dot{m}_{enriched\ oil}} \quad (5)$$

Where TPC represents the total plant cost, corresponding to the initial capital expenditure, given by the Total Equipment Cost (TEC), calculated from detailed components costs in 3.3 for the benchmark and in 4.4 for the membrane-based solution, and a fixed share for the installation (TIC), the indirect costs (IC) and the contingencies (C&OC). TPC is actualized using the first year Carrying Charge Fraction (CCF).

$$TPC = TEC \cdot \left(1 + \frac{\%TIC}{100}\right) \cdot \left(1 + \frac{\%IC}{100}\right) \cdot \left(1 + \frac{\%C\&OC}{100}\right) \quad (6)$$

Where the TEC is the sum of all components' costs, each one calculated from the relation:

$$TEC = \sum_k C_k \quad where \quad C_k = C_k^0 \cdot \left(\frac{S_k}{S_k^0}\right)^n \cdot \frac{CEPCI_{2024}}{CEPCI_y} \quad (7)$$

Where C_k^0 is the cost for the size S_k^0 at year y of each component k. Costs are reported to nowadays values using CEPCI method [31].

Operation and Maintenance (O&M) costs are divided in fixed (maintenance, insurance and labor) and variable (raw fish oil as feedstock, electricity and thermal energy).

Costs assumptions are reported, together with the description of variables for KPIs calculations, in Table 2.

Table 2: descriptions and values of KPIs

Variable	Units	Value	Comments
		Oil enrichment (OE)	
$x_{\omega 3,\, raw\ oil}$	−	31.65%	[26]
$x_{\omega 3,enriched\ oil}$	−	Calculated	It changes case-to-case
		Target recovery (TR)	
$\dot{n}_{EPA} + \dot{n}_{DHA}\vert_{raw\ oil}$	kmol/h	Calculated	Depends on inlet oil moles to achieve the desired target production
$\dot{n}_{EPA} + \dot{n}_{DHA}\vert_{enriched\ oil}$	kmol/h	Calculated	Depends on the product composition
		Specific energy consumption (SEC)	
$\dot{W}$	kW_{el}	Calculated	Estimated as 40% of $\dot{Q}$
$\dot{Q}$	kW_{th}	Calculated	Duty for reboilers in distillation columns
$\eta_{el,ref}$	kW_{el}/kW_{th}	0.45	[27]
$\dot{m}_{raw\ oil}$	kg/h	calculated	It changes case by case to meet production target
$\dot{m}_{enriched\ oil}$	kg/h	9.3	Set production to 10 L/h
		Specific GHGs emissions ($E_{CO_2,eq}$)	
GWP_{el}	g_{CO_2}/kW_{el}	352	[28]
GWP_{th}	g_{CO_2}/kW_{th}	201	[28]
$GWP_{raw\ oil}$	$g_{CO_2}/kg_{raw\ oi}$	1,760	Average between [29] and [30]
		Levelized cost of product (LCOP)	
TEC	k€	Calculated	Specific for each plant
$CEPCI_{2024}$	-	800	[32]
%TIC	-	65	[33]
%IC	-	14	[33]
%C&OC	-	15	[33]
TPC	**k€**	**Calculated**	
CCF	**1/y**	**0.16**	[33]
%Maintenance	-	2	Fixed share of TPC
%Insurance	-	2.5	Fixed share of TPC
labor	k€/y	30	[27]
$O\&M_{fix}$	**k€/y**	**Calculated**	**Maintenance + insurance + labor**
Raw fish oil	€/kg	10	[34]
Electricity	€/kWh_{el}	0.123	[28]
External heat	€/kWh_{th}	0.046	[28]
$O\&M_{var}$	**k€/y**		**Fish oil + electricity + heat in a year**
h_{eq}	h/y	7,200	[28]
LCOP	**€/kg**	**Calculated**	

Journal Pre-proofs

3. Benchmark process

3.1 Layout and assumptions

The layout for the benchmark fatty acid concentration system is shown in Figure 2. In the first step, triglycerides transesterification is performed to release the fatty acids from their glycerol backbone. The reaction is performed by mixing ethanol, refined crude oil and an alkali catalyst (NaOH, 10 g/L_{oil}[28]), at 60 °C and atmospheric pressure. Transesterification reactor converts each TAG in the corresponding EE with a yield of 73%, while remaining 27% of glycerides are in the form of DAGs or MAGs. Ethanol is fed at reactor inlet with an ethanol/oil molar ratio of 16 [28]. Excess of ethanol is recovered in a distillation column. Then, oil is pumped to water washing section, where remaining ethanol, glycerol and the catalyst are recovered, as well as TAGs and MAGs are totally removed. Water for washing is 14% of the inlet mass in the column [35]. Catalyst in aqueous solution reacts with H_3PO_4 to produce a salt (Na_3PO_4), that is removed using a filter. In a column, almost pure glycerol is separated from water and ethanol in the mixture. Oil, in form of EEs, from washing section, is then concentrated in the desired acids using molecular distillation (MD). In this process, ethyl ester fatty acids are separated by boiling point using high vacuum conditions (0.1-0.6 mbar). In the distillation unit, EEs lighter than EPA and DHA are mainly distilled, and an enriched oil is produced from the bottom of the column. Last step is another transesterification reactor where EEs are converted back to glycerides, reacting with glycerol and a selective enzyme. A conversion of 50% has been chosen for each EE, since this represents the lower limit to have a re-esterified TAG [10]. As a product of the reaction, ethanol is obtained, further separated in a column and then recirculated back.

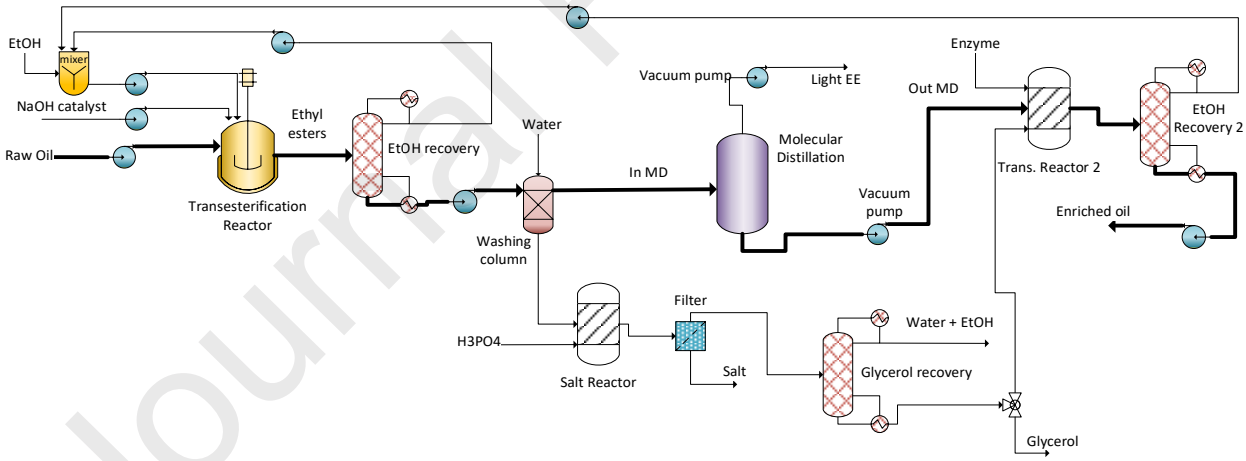

Figure 2: layout of the benchmark process for ω3 concentration. Oil is converted in an EE mixture, further concentrated in a molecular distillation section and then converted back to glycerides.

Reference case has been modelled using the software Aspen Plus®. Since not all the components of the fish oil are available in the Aspen properties database, all the acids have been grouped in 5 classes and for each class one acid is taken as representative component. The criterium has been to group the acids with the same number of carbon atoms, since this results with reasonable approximation in a similar ethyl esters boiling point [7] and therefore similar behavior in molecular distillation enrichment process and in distillation columns. In Table 3 are reported the components used in the simulation and the acids that each class represents. Final mixture will be enriched in acids of class C20 and C22. To find the enrichment in ω3 of the final mixture, it

should be considered that EPA represents 82.55% of acids in C20 class and DPA represents 86.28% of acids in C22 class.

Table 3: simplified oil model in benchmark. Acids are grouped in 5 classes according to their number of carbon atoms.

Raw oil composition				
Class	***Acid in the model***	***name***	***Real acids in the class***	***Mole fraction***
(-)	(-)	(-)	(-)	(%)
C14	C14:0	myristic	C14:0	10.87
C16	C16:0	palmitic	C16:0 / C16:1 / C17:0	33.15
C18	C18:1 cis 9	oleic	C18:0 / C18:1 cis 9 / C18:1 cis 11 / C18 :2 / C18 :3	18.28
C20	C20:4	arachidonic	C20:0 / C20:1 / C20:5	23.56
C22	C22:1	erucic	C22:1 / C22:5 / C22:6	14.14

In Aspen Plus, transesterification reactor is modelled using a Rstoich reactor at constant temperature and pressure, with specified final yield of 73% of TGs to EEs. Pumps are modelled by fixing discharge pressure and with an efficiency of 0.7. Washing column is a separator block with a unitary split fraction for all components beyond EEs. Salt reactor is a Rstoich block, where the reaction $3NaOH + H_3PO_4 \rightarrow NA_3PO_4 + 3H2O$ is performed with 100% conversion. Filter is a separator block with unitary separation of salt. MD is modelled as a flash unit, as described in detail in the next section. The second transesterification reactor is a Rstoich block where the conversion of EEs into TGs was set to 50% for all acids. Distillation columns are RadFrac blocks working at low pressures (0.1-0.4 bar), where reflux ratios and number of stages have been selected in every column by performing a sensitivity analysis. Both parameters were variated in order to achieve the desired component recovery, while limiting the maximum operating temperature at the reboiler at 170 °C to avoid thermal instabilities in the oil.

3.2 Molecular distillation modeling

Molecular distillation unit is the key component in the process for fatty acids enrichment. However, a block to model MD is not available in Aspen database. Therefore, an approach was selected from literature, taken from the work of Mallman et al. [36]. In that work, a flash vessel has been used in Aspen Plus, and the results compared to the ones obtained by a specific software for MD, named DISMOL. The flash was set at the same pressure, but it tuned out to have a different temperature in Aspen to reach the same distillate mass ratio D/F (i.e., mass of distillate over mass of feed). By defining a correction factor, given by the ratio between Aspen and DISMOL temperatures in Kelvin, and multiplying this factor for the target component molar fraction in the distillate, the authors managed to reproduce DISMOL results in terms of distillate amount and composition.

The same approach can in principle be applied also to fish oil MD. To verify that, the approach developed by Mallman et al. was validated by comparing the results of a flash unit in Aspen plus against experimental results of a two-stage MD enrichment of ω3 in fish oil, investigated by Rossi et al. [37]. Rossi et al. provide information about both stages' compositions and mass flows, operating at 40 Pa and investigating different temperatures. Due to the complexity of the fish oil mixture compared to the binary mixture used by Mallman et al., it has been decided in the validation to avoid using the correction factor on the distillate mass fractions,

since it would complicate too much the closure of mass balances. Moreover, being a two-stage molecular distillation with enriched product as distillate of the second unit, it is possible that the two correction factors compensate each other. Therefore, Aspen flash units have been operated at the same pressure of 40 Pa as experimental, while temperatures have been varied to reach the same distillate-to-feed mass ratio, while the ω3 enrichment has been verified a posteriori.

Initially, the first column has been investigated. In the experiments of [37], a mixture with 29.3% as mass fraction of ω3 was fed to the MD column at 100, 110 and 120 °C. Aspen temperatures to reach the same distillate-to-feed mass ratio were 139.5, 144.5 and 151.2 °C respectively. Comparison between mass fraction of ω3 in the experiments and computed by Aspen flash are reported in of Figure 3, left.

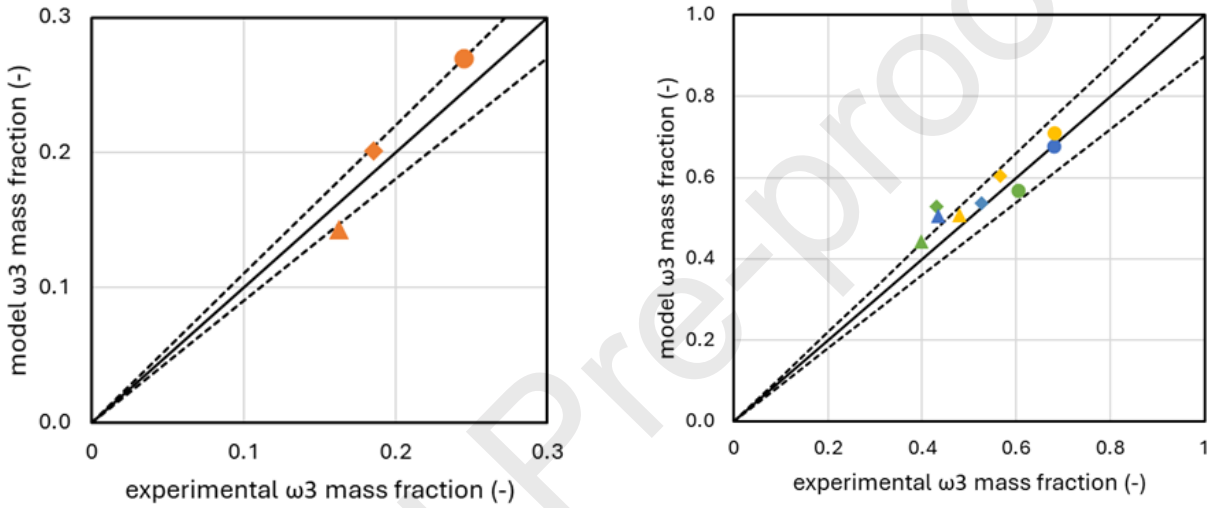

Figure 3: MD model validation. On the left, 1-stage MD validation. On the right, 2-stages MD validation (▲: first stage at 100 °C; ♦: first stage at 110 °C; ●: first stage at 120 °C; green: second stage at 120 °C; blue: second stage at 130 °C; yellow: second stage at 140 °C). Dashed lines are confidence bands at $\pm 10\%$

By setting these temperatures at the first stage, also the results of the second stage have been compared. Two-stage comparison is expected to be even more accurate than the single-stage, since potential overestimations of the ω3 computed by the model should be here underestimated. Results in terms of ω3 enrichment, for three temperatures at the first stage (100, 110, 120 °C) and for each of them three of the second stage (120, 130, 140 °C) are reported at the right side of Figure 3, showing that most predictions are in the range $\pm 10\%$. Temperature ratios were in most cases between 1.12 and 1.17, although in two cases resulted higher (about 1.35 – 1.37). Taking the median values, the first-stage ratio has been set to 1.09 and the second-stage ratio 1.16. Results of the MD validation are summarized in Table 4.

Table 4: experimental results from [37] and validation of the MD model. Model temperatures are set to obtain the same distillate/feed ratio, while ω3 fraction comparison is done to validate the model.

Experimental				***Model***			
Stage Temperature		***Final D/F***	$x_{\omega 3,out}$	***Flash Temperature***		***Final D/F***	$x_{\omega 3,out}$
1st	***2nd***			***1st***	***2nd***		
(°C)	(°C)	(-)	(-)	(°C)	(°C)	(-)	(-)
100	-	0.171	0.163	139.5	-	0.171	0.143

110	-	0.33	0.186	144.5	-	0.33	0.201
120	-	0.461	0.245	151.2	-	0.461	0.270
100	120	0.431	0.399	139.5	168.1	0.431	0.442
100	130	0.508	0.435	139.5	200	0.508	0.505
100	140	0.512	0.48	139.5	207	0.512	0.508
110	120	0.263	0.43	144.5	170.7	0.263	0.529
110	130	0.373	0.566	144.5	273	0.373	0.604
110	140	0.42	0.526	144.5	295.6	0.42	0.537
120	120	0.125	0.603	151.2	171	0.125	0.568
120	130	0.189	0.679	151.2	187.5	0.189	0.678
120	140	0.216	0.681	151.2	205	0.216	0.710

In conclusion, MD unit can be modelled using the flashes approach of Mallmann *et al.* [36], that has been here validated also for fish oil enrichment. This in general guarantees an accuracy within $\pm 10\%$, where the deviations can be attributed to the simplicity of the approach of Mallmann *et al.*, originally developed for a simple binary mixture and here applied to a more complex multicomponent system. Accuracy can be however considered suitable for the analysis. Flash column operates at the same pressure as the real MD column, while temperatures are freely variated and investigated in the software. The actual temperatures can be later found from Aspen flash temperatures by dividing the one of each column for the corresponding correction factor.

In the benchmark process of Figure 2, it is supposed that washing section fully removes TAGs and MAGs. Therefore, the feed of the MD unit is solely composed by EEs, where EPA and DHA are in the heaviest classes. In this case, a second stage is not needed, since there is no need to separate heavier components. MD is therefore modelled with a single flash unit, with temperature correction factor of 1.09.

3.3 Economics on equipment costs

Regarding economic assumptions on the equipment, components costs are reported in Table 5.

Table 5: equipment costs assumptions for benchmark process

Component	S_k^0	**Units**	C_k^0 (€)	**n**	**CEPCI$_y$**	**y**	**Ref**
Transesterification reactor	22.14	kg_{oil}/h	37,000	0.4	541.7	2016	[28]
Distillation column (3x)	55.75	kg_{in}/h	114,873	0.65	541.7	2016	[28]
Pumps + catalyst recovery + mixers	/	/	50,000	/	541.7	2016	[28]
Molecular distillation unit	0.03	kg_{in}/s	578,864	0.81	1000	/	[38]

4. Membrane-based process

4.1 Layout

The schematic of the membrane-based solution for ω3 fatty acids enrichment is represented in Figure 4. Ethanol-oil mixture is fed to a fixed-bed reactor, packed with immobilized CAL-A enzyme beads. While flowing along the reactor, oil and ethanol react, thanks to the lipase, such that short-chain acids are preferentially detached from the glycerol backbone of the TAGs. Reactor is kept at 40 °C and atmospheric pressure.

The mixture at the outlet of the reactor is then diluted with ethanol, to reduce its viscosity and facilitate membrane permeation, such that ethanol molar concentration in the mixture is 90% (about 50% in mass). Ethanol-oil mixture is then compressed and injected in the membrane module, also maintained at 40 °C. Ethanol (and glycerol produced in the reactor) easily crosses the membrane; the different esters are retained with different rejections, where EEs have the highest permeability. Therefore, in the permeate stream the oil fraction is enriched in EEs, while on the other side the retentate is enriched in glycerides. Since glycerides had been in turn preferentially enriched in ω3, the retentate, once removed ethanol in a distillation column, will be the final product. Permeation is facilitated by using ethanol as sweep flow, which reduces the concentration of the solutes and then the resistance to permeation. Permeate stream is then rich in ethanol, which is later separated in a distillation column, from which bottom exit a mixture of EEs and glycerol, with very similar boiling points, which can be later separated in a decanter.

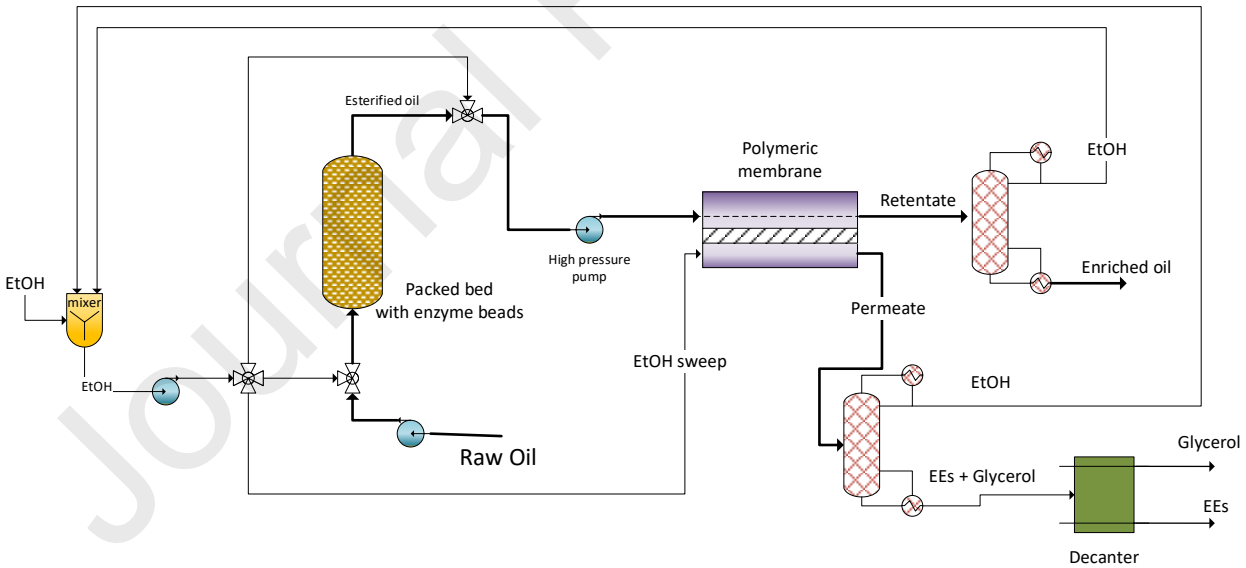

Figure 4: membrane-based process layout.

In Aspen Plus, both transesterification reactor and membrane section were modelled through customized developed Aspen Custom Modeler blocks, where the models developed are described in detail in sections 4.2 and 4.3 respectively. Pumps have a set output pressure and an efficiency of 0.7, while distillation columns are modelled through RadFrac columns, where, as in benchmark, reflux ratio and number of stages have been variated through a sensitivity analysis to recover ethanol while maintaining reboiler temperature below 170 °C. Decanter is modelled by a separator block that fully recovers glycerol.

4.2 Transesterification reactor model

4.2.1 Kinetic model

Kinetic model used for selective lipase-assisted transesterification is taken from another work of the same authors [26]. The model assumes that, in fish oil, all fatty acids are randomly distributed on the available positions on the glycerol backbones. This gives, assuming that behavior is not influence by the positions (sides or center) of the acid, (455 TAGs, since there are 13 acids detected in fish oil and their combinations in groups of 3 is considered). Each acid, when reacting with ethanol, is detached according to the three following consecutive reactions:

$$TAG + C_2H_5OH \leftrightarrow DAG + EE \quad \text{R.1}$$

$$DAG + C_2H_5OH \leftrightarrow MAG + EE \quad \text{R.2}$$

$$MAG + C_2H_5OH \leftrightarrow C_3H_5(OH)_3 + EE \quad \text{R.3}$$

Reaction rates (in mol/(h·g)) for the generic acid *i* are given by the relations:

$$rr_{i,\,R.1}(m_{enzy}) = \left.\frac{d\dot{n}_i^{EE}}{dm_{enzy}}\right|_{R.1} = \vartheta_{i,f} \cdot \dot{n}_i^{TG} \cdot \dot{n}_{EtOH} - \vartheta_{i,b} \cdot \dot{n}_i^{DG} \cdot \dot{n}_i^{EE} \quad (8)$$

$$rr_{i,\,R.2}(m_{enzy}) = \left.\frac{d\dot{n}_i^{EE}}{dm_{enzy}}\right|_{R.2} = \vartheta_{i,f} \cdot \dot{n}_i^{DG} \cdot \dot{n}_{EtOH} - \vartheta_{i,b} \cdot \dot{n}_i^{MG} \cdot \dot{n}_i^{EE} \quad (9)$$

$$rr_{i,\,R.3}(m_{enzy}) = \left.\frac{d\dot{n}_i^{EE}}{dm_{enzy}}\right|_{R.3} = \vartheta_{i,f} \cdot \dot{n}_i^{MG} \cdot \dot{n}_{EtOH} - \vartheta_{i,b} \cdot \dot{n}_{Gly} \cdot \dot{n}_i^{EE} \quad (10)$$

Where n_i^y are the mole flows of acid *i* in the ester form y in the mixture and m_{enzy} are the grams of enzyme beads; subscript *Gly* stands for glycerol and *EtOH* for ethanol. The parameters ϑ_i for the forward (f) and backward (b) reactions are functions of ethanol volumetric concentration based respectively on the relations:

$$\vartheta_{i,f} = k_{i,f} \cdot e^{a_{i,f} \cdot (0.09 - q)} \quad (11)$$

$$\vartheta_{i,b} = k_{i,b} \cdot e^{a_{i,b} \cdot (0.09 - q)} \quad (12)$$

Where q is the ethanol volumetric fraction in the mixture. Values of k_i and a_i are tabulated for 5 relevant fatty acids in Appendix.

Kinetic model has been developed in [26] for a batch process, therefore moles of esters evolve over time with a fixed amount of catalyst. This time-dependance of batch processes is here related to an enzyme dependance to be able to use the model in a flow process.

4.2.2 Reactor model assumptions

The fixed bed reactor is modelled as an isothermal reactor working in plug-flow behavior. Description is therefore 1D, and ethanol-oil mixture reacts along reactor length as the liquid flow encounters packed enzyme beads. Reactor works in steady state.

Once determined the mass of enzyme packed into the flow reactor, it would be possible to directly determine the volume of the reactor by assuming a value for beads density and void fraction inside the bed.
Material balances come from the integration of the following expressions:

$$\frac{d\dot{n}_i^{TAG}}{dm_{enzy}} = -\sum_{i=1}^{N} P_{z,i}^{TAG} \cdot rr_{i,\,R.1} \tag{13}$$

$$\frac{d\dot{n}_i^{DAG}}{dm_{enzy}} = \sum_{all\,TGs\;\delta} \psi_{DG}^{TG} \cdot rr_{j,\,R.1} \cdot P_{\delta,j}^{TAG} - \sum_{i=1}^{N} P_{z,i}^{DAG}(t) \cdot rr_{i,\,R.2} \tag{14}$$

$$\frac{d\dot{n}_i^{MAG}}{dm_{enzy}} = \sum_{all\,DGs\;\delta} \psi_{MG}^{DAG} \cdot rr_{j,\,R.2} \cdot P_{\delta,j}^{DAG} - \sum_{i=1}^{N} rr_{i,\,R.3} \tag{15}$$

$$\frac{d\dot{n}_i^{EE}}{dm_{enzy}} = rr_{i,\,R.1} + rr_{i,\,R.2} + rr_{i,\,R.3} \tag{16}$$

$$\frac{d\dot{n}_{EtOH}}{dm_{enzy}} = -\sum_{i=1}^{N} rr_{i,\,R.1} - \sum_{i=1}^{N} rr_{i,\,R.2} - \sum_{i=1}^{N} rr_{i,\,R.3} \tag{17}$$

$$\frac{d\dot{n}_{Gly}}{dm_{enzy}} = \sum_{i=1}^{N} rr_{i,\,R.3} \tag{18}$$

Where i indicates each fatty acid, that can be in the form k = TAG, DAG, MAG or EE specified in superscript. In DAG and MAG balances it also appears the terms ψ_{DG}^{TG} and ψ_{MG}^{DAG}, which is a Boolean variable (with value 1 or 0) introduced to evaluate if a specific DAG (or MAG) can be obtained by the upper TAG (or DAG) δ: the value is 1 if it can be obtained, zero if not. The terms $P_{z,i}^{k}$ are the probability of detachment, that states that the probability to detach acid i from the component z, that is a ester of type k, is given by the ratio between the moles of acid i in that component over the total moles of acid i in all components within the same ester type.

$$P_{z,i}^{k} = \frac{\dot{n}_{z,i}^{k}}{\sum_{all\;z\;in\;k} \dot{n}_{z,i}^{k}} \tag{19}$$

More detail about the mathematical model can be found in [26].

4.3 Membrane permeation model

4.3.1 Transport model

Each chemical component permeates through the polymeric membrane with a molar flux given by the solution-diffusion model, as reported in Peeva *et al.* [23]. Derivation of flux equation is reported in Appendix B.

$$j_y = \wp_y \cdot \left[x_{y,ret} - x_{y,per} \cdot exp\left(-\frac{v_{mol,y} \cdot \Delta P}{R \cdot T} \right) \right] \tag{20}$$

Where j_y is the molar flux $\left(\frac{mol}{m^2 \cdot h}\right)$, $\wp_y$ is the component permeability $\left(\frac{mol}{m^2 \cdot h}\right)$, $x_{y,r}$ and $x_{y,p}$ are the molar fractions of the component at the retentate-side and at the permeate-side of the membrane. Exponential term includes molar volume, transmembrane pressure, universal gas constant and temperature.

In this formulation of the model, for components it is meant TAGs, DAGs, MAGs, EEs and ethanol. It is thus assumed that the membrane does not make distinctions among the different acids, and then the separation occurs only based on the ester form of the component. To make an example, permeability of EEs is the same for EPA-EE or myristic acid EE, or any other acid that is found as EE. This assumption is due to the high number of different combinations of components in the mixture, which would have made very complex the determination of the membrane selectivity to all of them.

Permeabilities have been determined experimentally, and their determination is described in section 4.3.2. Components molar fractions evolve along the membrane, as part of the mixture permeates. Their value is determined by the material balances computed by the model, described in section 4.3.3. Molar volumes assumed for the different components are reported in Table 7.

4.3.2 Experimental determination of components permeabilities

The permeabilities of all components have been determined in a series of experiments performed at VITO facilities, where a mixture of ethanol and the ester of interest has been prepared for each ester. The reference compounds were the esters of oleic acid. As these reference compounds are typically only available in small quantities, experiments have been run in very diluted conditions (about 0.5 g of solute in 1 L ethanol) and using a flat sheet membrane of surface area 100 cm^2. Experiments are summarized in Table 6.

Table 6: experiments to determine components permeabilities.

Experiment number	Feed	Solute concentration	Purpose	Samples taken
1	Ethanol and glyceryl trioleate	0.5 g in 1 L ethanol	Determine TAGs permeability	3x3
2	Ethanol and dioleylglycerol	0.5 g in 1 L ethanol	Determine DAG permeability	3x3
3	Ethanol and 1-oleyl-rac-glycerol	0.5 g in 1 L ethanol	Determine MAG permeability	3x3
4	Ethanol and ethyl oleate	0.5 g in 1 L ethanol	Determine EE permeability	3x3
5	Ethanol, glyceryl trioleate, 1-oleyl-rac-glycerol and ethyl oleate	0.6 g (0.2 g for each solute) in 1 L ethanol	Model validation	3x3

Experimental membrane process was a batch process in cross flow configuration, where the ethanol-oil mixture is stored in a feed tank, from where it is pumped over the membrane with a cross flow velocity of 0.3 m/s, that divides the stream in a permeate flow, stored in another tank, and in the retentate flow, that is recirculated back to the feed tank. Samples were taken from both feed tank, permeate point (i.e. the permeate flowing in a given time from the membrane) and permeate tank (that in a given time is the results of the history of permeation) to be able to have a closure of material balances and then determine the flux of solvent and

solute (when referring to "one sample" it means one pressure and one time, sampling in three different positions). Experiments were run at 40°C and at three different transmembrane pressures (10, 20 and 30 bar); three samples were taken for each pressure at 3 different times (after about 100, 200 and 300 minutes of experiment). After taking the three samples at each pressure, all permeate is returned to the feed tank to minimize any effects of solution concentration on membrane performance. Thus, 9 values of the permeability are available for each component (plus ethanol permeability, which can be verified from all samples). Commercial polymeric membrane Borsig oNF-1 has been purchased from BORSIG membrane Technology GmbH [39], a Thin Film Composite (TFC) membrane, with a dense low polarity selective layer over a porous support. Though Borsig membranes do not require preconditioning all membranes were cleaned by permeating a small volume of ethanol through the membrane prior to use. Experimental setup is reported in Figure 5.

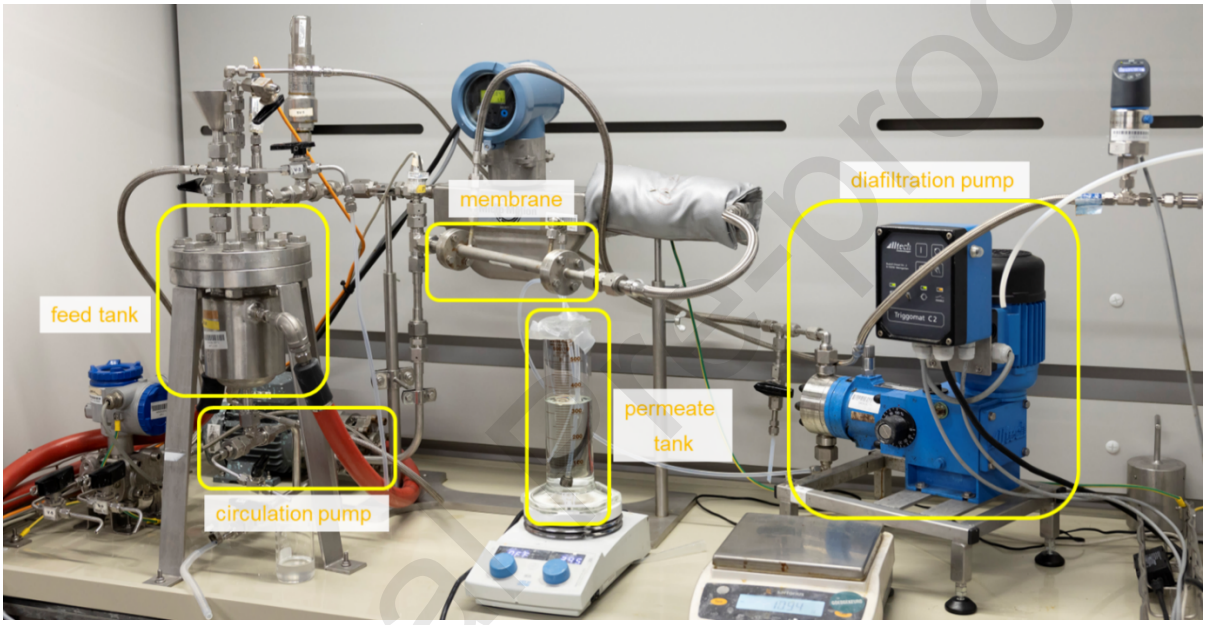

Figure 5: experimental setup, in VITO facilities, for permeabilities determination.

Experimental results on permeability values are reported in Figure 6. As expected, the EE permeability is higher than the ones of the other esters, as the purpose of the membrane process in indeed to separate the EEs fraction, depleted in the ω3 fatty acids. Their average values are taken as values in the model, also summarized in Table 7. EEs permeability turned out to be 4,985.9 mol/(m^2·h), for TAGs 840.8, for DAGs 346.3 and for MAGs 199.6. These values suggest that, beyond components size, also polarity has an effect, since among the glycerides TAGs turned out to be the most permeable. Ethanol permeability, reported on the right chart of Figure 6, could be determined from each of the experiments. Being ethanol the solvent of the mixture, its permeability turned out to be a function of the transmembrane pressure, and therefore it is not possible to define a constant value to be used in equation (20). Ethanol permeability is although defined in the range of interest (10-30 bar) by linearly interpolating the experimental values.

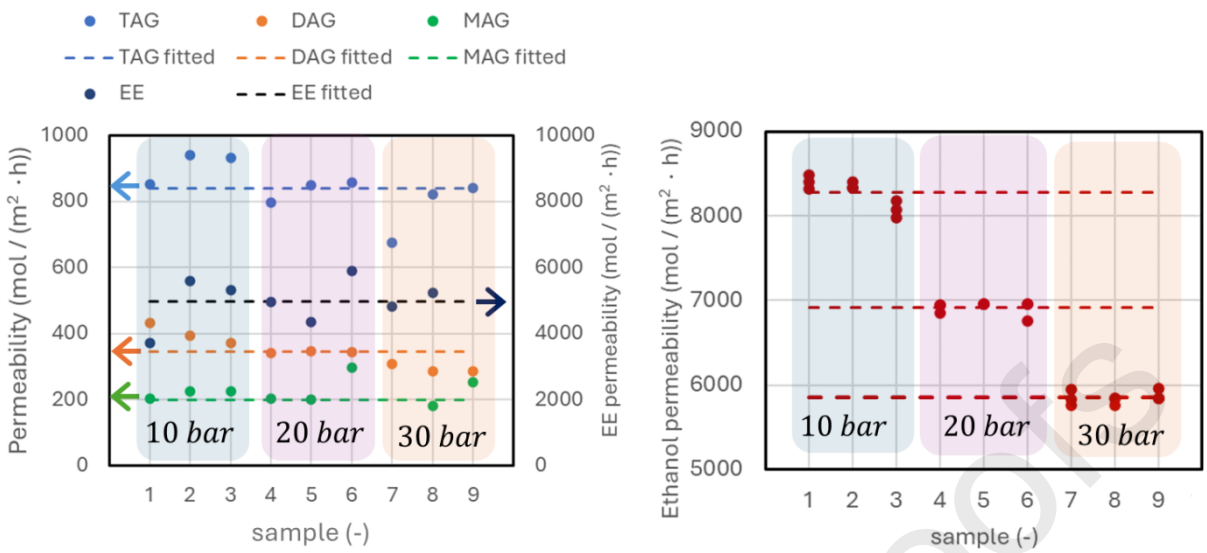

Figure 6: experimental results for determination of esters permeabilities.

The permeabilities defined so far have been determined for one reference acid (oleic acid), but it is assumed that this might be representative of all the acids in the same ester form. Moreover, they have been derived from experiments where each ester was in the mixture with only ethanol. The validation of the model was performed by running an experiment where the reference components (excluding DAGs, which were not available) were mixed together in the ethanol solution. In other words, validation aimed to verify that also the behavior in mixture could be represented by the same permeability values. Results of the validation experiment, also performed at 10, 20 and 30 bar with 3 samples taken at different time for each pressure, are reported in Figure 7. Fitted permeation values used in the model were able to predict the experimental values determined in the validation experiment. For EE, some outliers have been observed, possibly due to measurements issues or non-negligible solvents interactions. Model permeability is in any case lower compared to these measured values, and therefore the model is conservative in their predictions. This means that eventually it underestimates membrane performance.

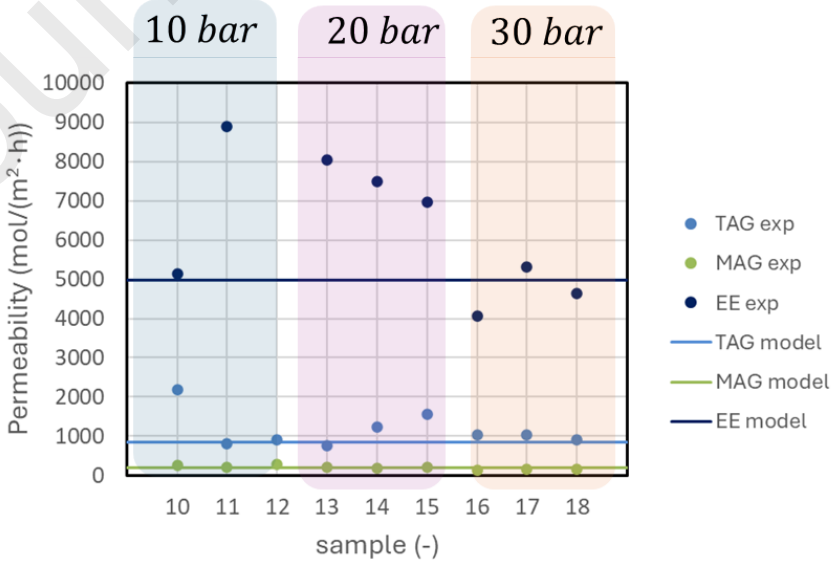

Figure 7: validation of permeation model for a reference component mixture in ethanol.

Permeabilities, together with molar volumes to be used in the transport model equation, are summarized in Table 7. These values, although determined experimentally only for very high dilutions in ethanol, will be assumed to be valid also at lower ethanol fractions, and in general in all conditions where membranes are investigated.

Table 7: assumptions for SD permeation model

Component	Average molar volume	Permeability $\wp$
	m^3/mol	$mol/(m^2 \cdot h)$
Ethanol	$5.90 \cdot 10^{-5}$	$9{,}446.1 - 121.48 \cdot \Delta P$
TAG	$9.85 \cdot 10^{-4}$	840.8
DAG	$6.83 \cdot 10^{-4}$	346.3
MAG	$3.80 \cdot 10^{-4}$	199.6
EE	$3.63 \cdot 10^{-4}$	4,985.9
Glycerol	Assumed that behaves as ethanol in permeation process, therefore included in the share of ethanol	

4.3.3 Membrane module assumptions

Purpose of the membrane separation process is to remove mainly the EEs, depleted in the target components, and to retain all glycerides (TAGs, DAGs, MAGs), where EPA and DHA are concentrated. The retentate flow after the membrane module, once excess ethanol is removed, represents the enriched oil target product.

The feed stream coming from the reactor is a partially-transesterified oil - where the glyceride (TAG, DAG, MAG) fraction is enriched in ω3 fatty acids while EEs are mostly the other acids – ethanol and glycerol. Ethanol fraction at the outlet can be very low, leading to a quite viscous solution which finds difficult to permeate through the membrane. For example, 9% ethanol volume fraction at the reactor inlet corresponds to 8% as mass fraction and 62% as mole fraction. As the reaction proceeds, ethanol reacts with fatty acids and therefore its fraction is reduced, increasing also mixture viscosity. The amount depends on the reaction time, but in general for the cases of interest ethanol molar fraction at the outlet is about 13% (1.5% as mass fraction). To reduce mixture viscosity and then to facilitate the permeation through the membrane, pure ethanol is added to the mixture after the reactor. In this work, it is assumed that in all cases ethanol is added to achieve 90% molar fraction of ethanol at membrane inlet. In this calculation, glycerol produced in the reactor is included in the ethanol share, since it is expected that it also crosses the membrane as easily as ethanol. Corresponding mass fraction, which depends also on glycerides conversion in the reactor, is around 50%.

To summarize, at the membrane inlet there is always a mixture of ethanol and oil, where ethanol is 90% molar and oil is 10%. Oil is composed by different fractions of TAGs, DAGs, MAGs and EEs depending on reaction conditions. Also dependent on reaction conditions is the amount of ω3 fatty acids in each ester.

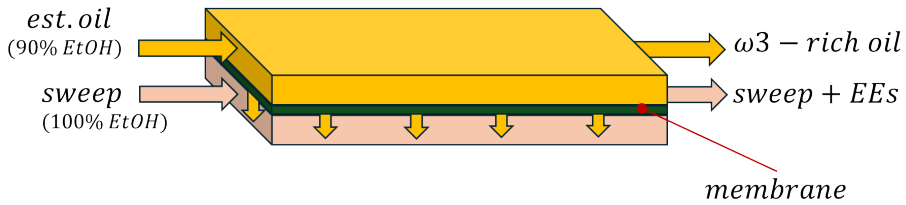

Figure 8: membrane modules layout assumed. Esterified oil is enriched as EEs permeate more selectively than other esters.

Membrane module in steady state conditions is represented in Figure 8 and it is described by a 1D model based on material balances, while considering uniform temperature (40 °C) and transmembrane pressure (20 bar). On the permeate side, pure ethanol is used as a sweep fluid, aiming to reduce the molar fraction of the EEs and therefore to facilitate their permeation. Different sweep fluid flow rates are studied to investigate their impact on membrane performance. Material balances for retentate-side and permeate-side are described by the following Cauchy's problems:

$$\begin{cases} \dfrac{d\dot{n}_{y,ret}}{dA} = -j_y = -\wp_y \cdot \left(\dfrac{\dot{n}_{y,ret}}{\sum_y \dot{n}_{y,ret}} - \dfrac{\dot{n}_{y,per}}{\sum_y \dot{n}_{y,per}} \cdot \exp\left(-\dfrac{v_{mol,y} \cdot \Delta P}{R \cdot T}\right)\right) \\ \dot{n}_{y,ret}(0) = \dot{n}^0_{y,ret} \end{cases} \tag{21}$$

$$\begin{cases} \dfrac{d\dot{n}_{y,per}}{dA} = j_y = \wp_y \cdot \left(\dfrac{\dot{n}_{y,ret}}{\sum_y \dot{n}_{y,ret}} - \dfrac{\dot{n}_{y,per}}{\sum_y \dot{n}_{y,per}} \cdot \exp\left(-\dfrac{v_{mol,y} \cdot \Delta P}{R \cdot T}\right)\right) \\ \dot{n}_{y,ret}(0) = 0 \qquad for\ y = TAG, DAG, MAG, EE \\ \dot{n}_{y,ret}(0) = \dot{n}_{sweep} \qquad for\ y = ethanol \end{cases} \tag{22}$$

An example of permeation and composition trends along the membrane is reported in Figure 9.

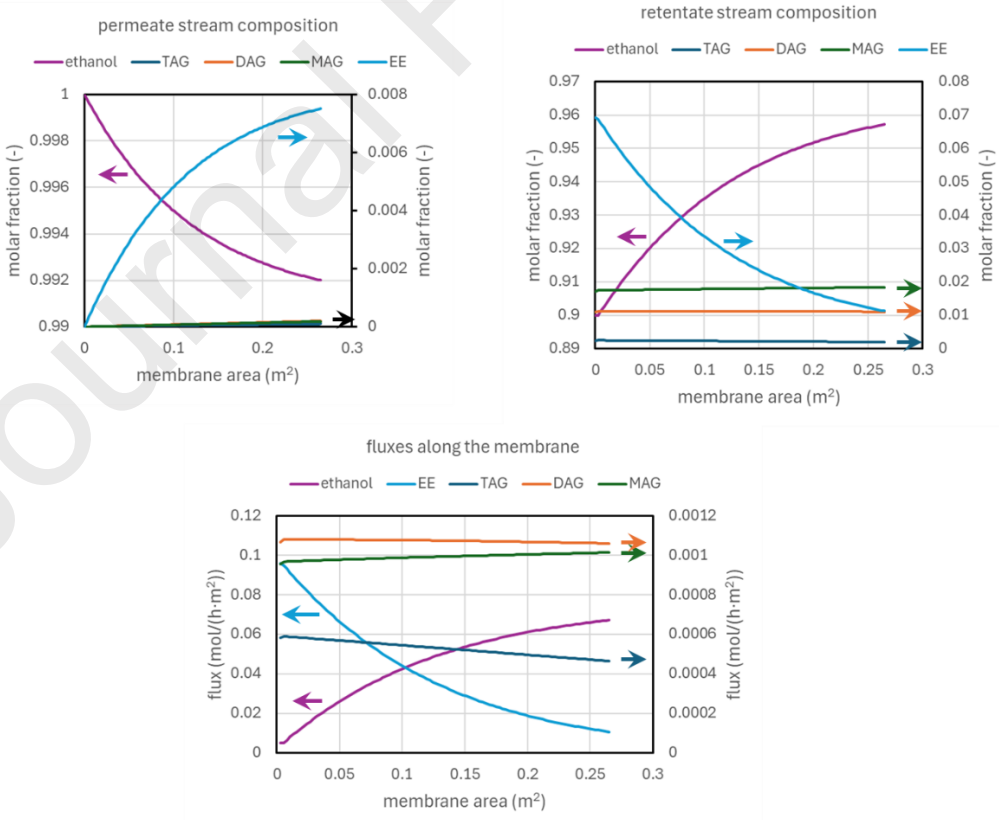

Figure 9: trends of molar fractions in permeate and retentate along the membrane, and fluxes for the different components. Feed composition: 90% CH_3OH, 0.25% TAG, 1.11% DAG, 1.72% MAG, 6.92% EE. Membrane area is totally 0.265 m². Sweep flow is 5 kmol/h; transmembrane pressure is 50 bar.

4.4 Economics

Membrane-based process share most of its economic assumptions with the benchmark process, and in general most of the values and the methodology procedure are the ones summarized in Table 2.

Beyond that, there are specific components that are only relevant in the membrane-based process, as obviously the cost of the membrane module itself. High pressure pump cost about 15 k€ and, together with enzyme beads, mixers and other pumps, it is assumed to be included in the 50 k€ of costs for auxiliaries. All relevant costs are summarized in Table 8.

Table 8: equipment costs assumptions for membrane-based process

Component	S_k^0	units	C_k^0 (€)	n	$CEPCI_y$	y	Ref
Polymeric membrane	1	m^2	5,078.4	1	1000	/	[38]
Distillation column (2x)	55.75	kg_{in}/h	114,873	0.65	541.7	2016	[28]
Pumps + enzyme + mixers + decanter	/	/	50,000	/	541.7	2016	[28]

5. Results and discussion

5.1 Benchmark process: techno-economic study

Benchmark plant is designed to produce an oil made by 31.845 mol/h of fatty acids, which is enriched in the EPA and DHA content. The enrichment depends on MD operating conditions (pressure and temperature):. A more enriched oil is desired since it corresponds to a more valuable product. On the other hand, in general high enrichment is obtained also with a higher loss of ω3, meaning, in the assumption to work at fixed production, a higher raw oil input, then a higher cost and higher auxiliaries' consumption. All other plant components (transesterification reactor, washing section, distillation columns) are assumed to work at fixed performance using literature assumptions, mainly based on the experiments of Fiori et al. [28] to optimize oil enrichment process performance. Raw oil flow rate is variated in all cases in order to reach target enriched oil production.

A sensitivity analysis has been performed changing the MD temperature, while maintaining pressure at 0.4 mbar, since it is an average value in MD operating range and is consistent with [37]. Results, in terms of OE and TR, are reported in **Figure *10***a. The dots indicated the simulations results. The same information is summarized in the TR-OR chart of in **Figure *10***b, with the corresponding value above each point representing its operating temperature (already scaled by factor 1.09). Even without enrichment, 27% of ω3 are lost due to incomplete conversion of TAGs in EEs in the reactor, and therefore are washed as DAGs and MAGs. This is visible as TR is 0.73 even when there is no enrichment. As MD temperature is increased, it is possible to obtain a more enriched product, while more ω3 are inevitably lost in the light EE distillate fraction of MD.

a

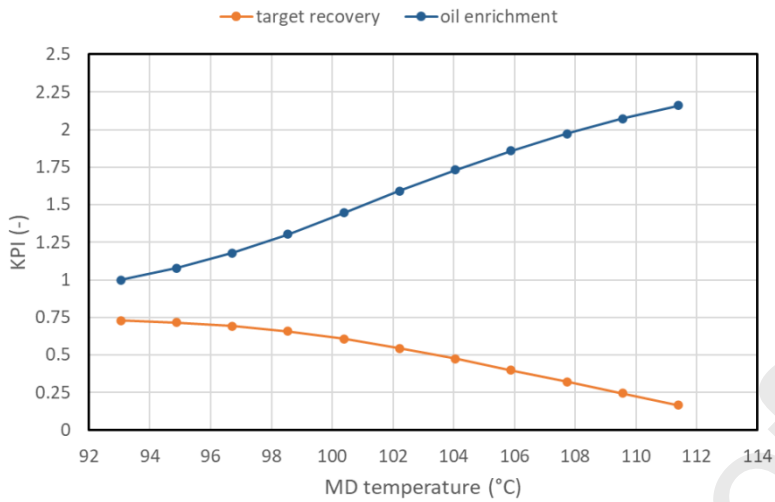

b

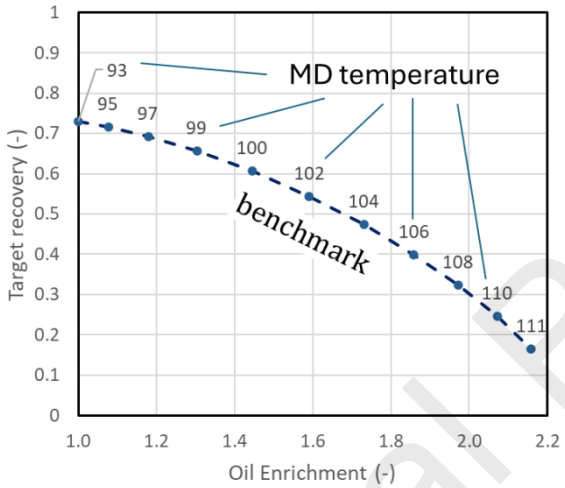

C

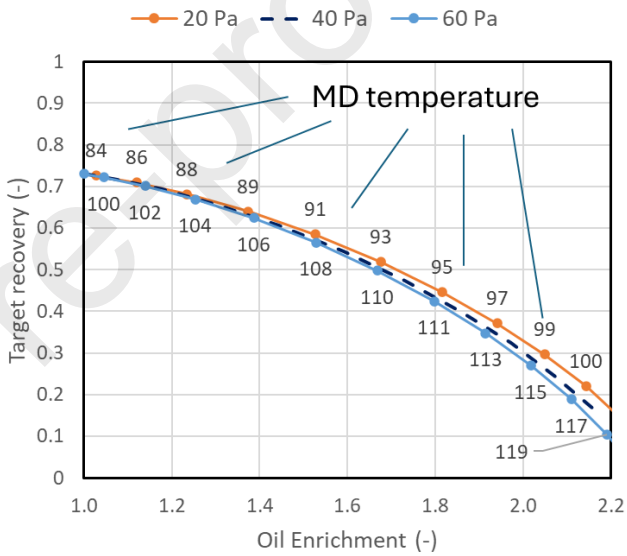

Figure 10: effect of MD temperature (top and left) at 40 Pa and effect of MD pressure (right) at different temperatures on oil enrichment and target recovery. A richer oil can be obtained by losing more ω3.

On the right side of **Figure *10***, the effect of operating pressure at different temperatures. Pressures investigated are 20, 40 and 60 Pa. Effect on performance is in general quite limited (a small gain can be detected at lower pressures). As pressure increases, also MD temperature increases to have a certain enrichment.

To have an idea of the streams flow rates and compositions, results for one of the cases analyzed are reported in additional materials.

5.2 Membrane-based process: techno-economic study

In the benchmark process described in the previous section, the reactive section it is assumed to convert, without any specific selectivity, all acids in the corresponding esters with a conversion of 73%. This means that the process performance in terms of enrichment and recovery of ω3 depends on how MD section is operated. In the membrane-based process, there is the additional degrees of freedom that both reactor and membrane can be regulated. Reactive part, based on the amount of lipase and on ethanol volumetric fraction,

determines the composition of the stream fed to the membrane; afterwards, membrane area and transmembrane pressure determine consequently the composition of the final product.

Therefore, the reactive section will be firstly analyzed in 5.2.1, and later coupled with the membrane in section 5.2.2. In membrane-based process, temperature is always assumed constant, and raw oil composition is fixed. Parameters investigated for the reactive part is the enzyme amount, which determines the outlet composition from the reactor. For the membrane section, permeabilities are assumed constant to the determined experimental values, while inlet composition, transmembrane pressure, sweep ethanol flow rate ad membrane area are analyzed. In all cases, enriched oil production is fixed, and raw oil flow rate is variated accordingly to reach target production.

5.2.1 Transesterification reactor results

When ethanol reacts with fish oil in presence of a selective lipase, short-chain acids are selectively detached from the glycerol backbone and converted to ethyl esters, while ω3 acids are left as much as possible attached to the glyceride. To evaluate the performance of the reactive section, it is still possible to use the parameters OE and TR. However, in doing so, it should be clear that the product mixture is not enriched "in itself", since glyceride fraction (enriched in ω3) and EEs (depleted in ω3) are still in the same mixture. When studying the reactor only, OE refers to the enrichment of the glyceride fraction (i.e. molar fraction of EPA+DHA in the glycerides over their molar fraction in the initial oil) and TR to the share of EPA+DHA that are still attached to the glycerol backbone. To specify this difference compared to the OE and TR of the final product of the process (i.e. after the separation section), the subscript *id* is added. Indeed, these values are the enrichment and recovery values that could be *ideally* obtained using a perfectly selective membranes, which has 100% rejections on all glycerides (TAG, DAG, MAG) and removes 100% of EEs. Using such a membrane it would be ideally possible to remove all the ethanol and all the EEs, leaving only pure glyceride fraction with an oil enrichment OE_{id} and a target recovery TR_{id}.

OE_{id} and TR_{id}, given the initial oil composition reported in Table 1, depend on the ethanol volumetric fraction and on the enzyme amount in the reactor. Curves obtained by variating these two parameters are reported in Figure 11, where it is also reported the line for the benchmark process. These results allow to understand the ideal process performance that could be obtained by an ideal membrane. Curves at different ethanol fractions overlap, while more ethanol means a higher maximum oil enrichment achievable. From the technical point of view, it is therefore possible to use the curve at 15%, since has a broader range of OE while having the same performance of the lower fractions.

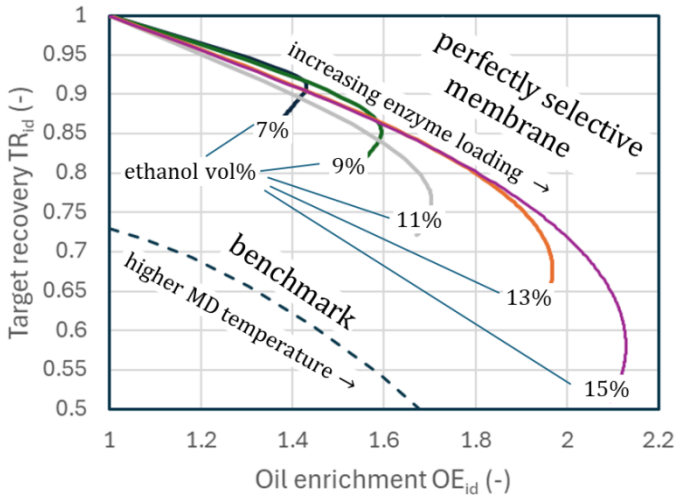

Figure 11: reactor section results, corresponding to the OE-TR that can be obtained with a perfectly selective membrane (100% rejection of TAG, DAG and MAG).

The transesterification reaction can be stopped at any OE_{id} by tuning the enzyme amount. Each enrichment corresponds to a different oil composition in terms of TAG, DAG and MAG fractions, and a different content in ω3 of each ester. Different esterified oil compositions are summarized in Table 9, and show as more enzyme is loaded the higher conversion to EEs, from one side (then lower TR) and the higher fraction of ω3 in the glycerides (higher OE).

Table 9: compositions of stream at the membrane inlet (i.e. coming from the reactor and then diluted with ethanol up to 90% molar fraction) for different extents of the reaction. Ethanol volume fraction at the reactor inlet is 15%.

OE_{id}	Ideal ω3 product fraction	TR_{id}	Molar fraction (relative to total esters, 10% of the total)				ω3 share (ω3 moles over total acids moles)			
			TAG	DAG	MAG	EE	TAG	DAG	MAG	EE
1.1	34.5%	0.980	55.6%	18.9%	2.1%	23.4%	34.5%	34.5%	34.5%	6.1%
1.2	38.1%	0.955	30.9%	24.2%	6.3%	38.6%	38.1%	38.1%	38.1%	6.9%
1.3	41.1%	0.935	20.6%	23.9%	9.3%	46.1%	41.1%	41.1%	41.1%	7.3%
1.4	44.0%	0.913	13.9%	22.1%	11.9%	52.1%	44.2%	44.3%	44.2%	8.0%
1.5	47.6%	0.886	9.4%	19.7%	13.9%	57.0%	47.6%	47.7%	47.5%	8.8%
1.6	50.5%	0.862	6.9%	17.6%	15.1%	60.4%	50.5%	50.6%	50.3%	9.5%
1.7	53.9%	0.832	4.8%	15.1%	16.2%	63.9%	54.0%	54.1%	53.5%	10.4%
1.8	56.9%	0.802	3.5%	12.9%	17.1%	66.5%	57.2%	57.6%	55.6%	11.4%
1.9	60.3%	0.763	2.5%	11.1%	17.2%	69.2%	60.5%	60.8%	59.0%	12.4%
2.0	63.4%	0.717	1.6%	8.9%	17.4%	72.0%	64.6%	64.8%	61.6%	14.0%
2.1	66.5%	0.646	0.9%	6.6%	17.4%	75.1%	69.6%	69.6%	63.6%	16.2%

These compositions represent the inlet conditions to the membrane section, and it is difficult to state *a priori* which is the best one to be adopted, since it depends on the reaction-membrane coupling, as discussed in the next section.

5.2.2 Process results after permeation

Membrane performance might depend on several factors: membrane area (per unit feed flow rate), mixture composition, operating pressure and sweep ethanol flow rate. An increase of membrane area, in general, leads to a higher oil enrichment (since EEs preferentially cross the membrane) but also to a lower recovery, for two

reasons: one is that the ω3 contained in the EE fraction inevitability are removed as EE are removed, and the second is that also some TAG, DAG and MAG crosses the membrane, bringing some ω3 on the permeate side. This trade-off reaches typically a maximum, when EE flow across the membrane goes to zero and then additional area would lead to a reduction in recovery and also a reduction in enrichment. All curves will be reported for different membrane areas to show this effect.

Transmembrane pressure (i.e. pressure of the retentate side minus pressure of the permeate side, assumed at 1 bar) has a limited effect on membrane performance, as reported for one case study in **Figure *12***a. It is however important to consider that while feed has 90% molar content of ethanol, sweep ethanol on the other side of the membrane is, at the beginning, 100% ethanol. It means that to allow ethanol always to flow from retentate to permeate side, it should be valid:

$$j_{EtOH} > 0 \rightarrow x_{EtOH,ret} - e^{\left(-\frac{v_{mol,EtOH}\cdot \Delta P}{R\cdot T}\right)} > 0 \rightarrow \Delta P > -\frac{R\cdot T\cdot \ln(x_{EtOH,ret})}{v_{mol,EtOH}} = 46.5\ bar$$

Where the value is obtained at 40 °C and using 0.9 as ethanol molar fraction, corresponding to inlet value, since it is observed that in all cases ethanol fraction at the retentate side increases as it goes through membrane area, due to the fact that EEs relatively permeates much more than ethanol. In all simulations, pressure difference is therefore set to 50 bar to always guarantee the ethanol positive flow.

Fixed operating pressure, another analysis is performed to study the influence of the inlet composition coming from the reactor. Different conditions are compared for the different OE_{id} reported in Table 9. For the comparison, it is assumed an infinite dilution in the permeate side (i.e. infinite sweep ethanol flow). Results are reported in **Figure *12***b. It can be observed that, in general, higher ideal enrichments allow to obtain higher real enrichment of the retained mixture, which in the best case reaches asymptotically the ideal value. In general, higher ideal enrichment allows, for a given real OE, a higher TR, and therefore a lower oil consumption. This is true up to OE_{id}=1.9. Beyond this value, it can be observed how curve at OE_{id}=2 has in general lower TR than the curve at OE_{id}=1.9. This effect is even more important if OE_{id} continues to increase. This leads to the conclusion that a OE_{id}=1.9 is the best design composition for the membrane section inlet.

Fixed pressure and composition (ΔP is set to 50 bar, and the composition is the one obtained by operating the reactor up to OE_{id} of 1.9), last analysis is the influence of sweep ethanol flow rate. While in general feed pump and enzyme beads has a low impact on the plant cost, and therefore it makes no difference at the end of the day if pressure is slightly higher or lower, or if the enzymatic reactor is a bit bigger or smaller, sweep flow directly affects the distillation column to recover the ethanol, that can be a major factor in final cost. For this reason, sweep ethanol flow will be studied both for its influence on the performance but also as a variable in the definition of oil production cost. Performance analysis is reported in **Figure *12***c. Sweep liquid aims to decrease molar fraction of solutes into the permeate side, increasing therefore their flux. It is therefore always convenient, from the membrane point of view, to increase the sweep flow rate. In the chart, it is reported also the ideal line with an infinite sweep flow rate (i.e., no resistance from the permeate side to permeation). Although ideal from the membrane point of view, an infinite sweep flow rate would mean an infinite distillation column to recover the ethanol, and basically infinite costs.

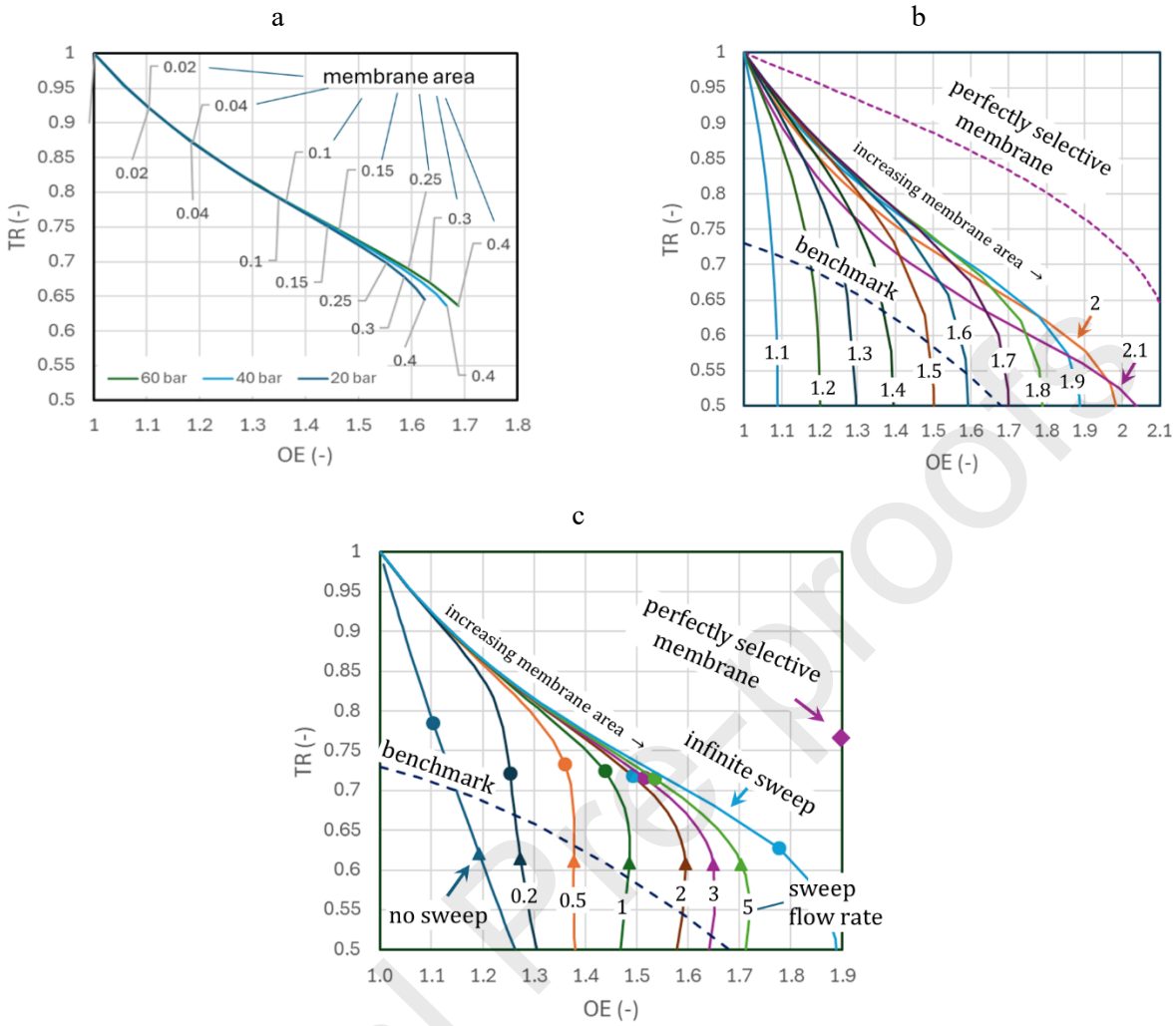

Figure 12: influence of: transmembrane pressure (a, in labels membrane area in m², sweep flow set to 5 kmol/h, OE_{id}=1.9) and inlet composition (b, in labels the OE_{id}, pressure 50 bar, infinite sweep flow rate), sweep flow rate (c, in labels sweep flow rate in kmol/h, pressure set to 50 bar, OE_{id}=1.9. ● indicates the points at 0.2 m² of membrane area; ▲ the points at 0.5 m²), all evaluated as functions of oil enrichment, by changing membrane area.

To summarize the results of the membrane section analysis, it can be stated that: (i) transmembrane pressure is set to 50 bar to guarantee in all cases a flux of ethanol from the retentate to the permeate side; (ii) reactor-membrane coupling has in general a higher TR by stopping the reaction when OE_{id} is 1.9. Inlet membrane stream composition (after mixing with pure ethanol up to 90% molar) results the following: 90% CH_3OH, 0.25% TAG, 1.11% DAG, 1.72% MAG, 6.92% EE. Desired final enrichment can then be determined changing membrane area. (iii) higher sweep ethanol flow rate is preferred from the membrane performance point of view, but it might lead to a severe increase in plant cost. Therefore, it should be optimized from an economic point of view. This is done in the next section.

5.3 Economic comparison

Based on the considerations of the previous section, economic comparison is done considering the benchmark against membrane-based solution, where the latter is operated: (i) with a 15% ethanol volumetric fraction at the inlet of the reactor; (ii) enzymatic reaction is performed such that the oil is enriched up to OE_{id}=1.9, with

the corresponding composition of Table 9; (iii) ethanol is added after the reactor to reach a molar fraction of 90%; (iv) ethanol-oil mixture is compressed up to 51 bar. In this situation, membrane area and sweep ethanol flow rate, and in turn membrane performance and distillation column to recover the ethanol, are considered as variables of the economic analysis.

Economic methodology has been presented in section 2.3, with equipment costs reported in 3.3 for the benchmark and in 4.4 for the membrane-based process. LCOP is specific to one kg of final product. As stated in 2.2, all systems produce 31.845 mol/h of fatty acids, that would correspond to 10.615 mol/h of TAGs and then about 9.3 kg/h, that are about 10 L/h. For the calculation of the yearly production of enriched oil, 7,200 hours of yearly operations are assumed.

Results of economic comparison is reported in Figure 13, where product cost using benchmark is compared to the cost using the membrane-based process, assuming to use sweep flow at different flow rates. With both plants it is possible to tune the desired enrichment level, while a higher enrichment is always associated with a higher product cost mainly due to higher raw oil input required. Membrane-based process is in all cases convenient, and it turns out that the lower the sweep flow, the lower the cost. However, consistently with results in Figure 12c, lower sweep flow rates put a cap on the enrichment that can be achieved, close to which the cost has a steep increase. Therefore, using 0.2 kmol/h of flow rate it is convenient only for OE up to 1.2; 0.5 kmol/h is convenient up to OE=1.3; 1 kmol/h is convenient up to OE=1.45; 2 kmol/h up to OE=1.55; 3 kmol/h up to OE=1.6 and 5 kmol/h up to 1.72. To obtain higher enrichments it would be necessary to go back to the enzymatic reaction and increase the OE_{id}, using a new composition and calculating again the process costs.

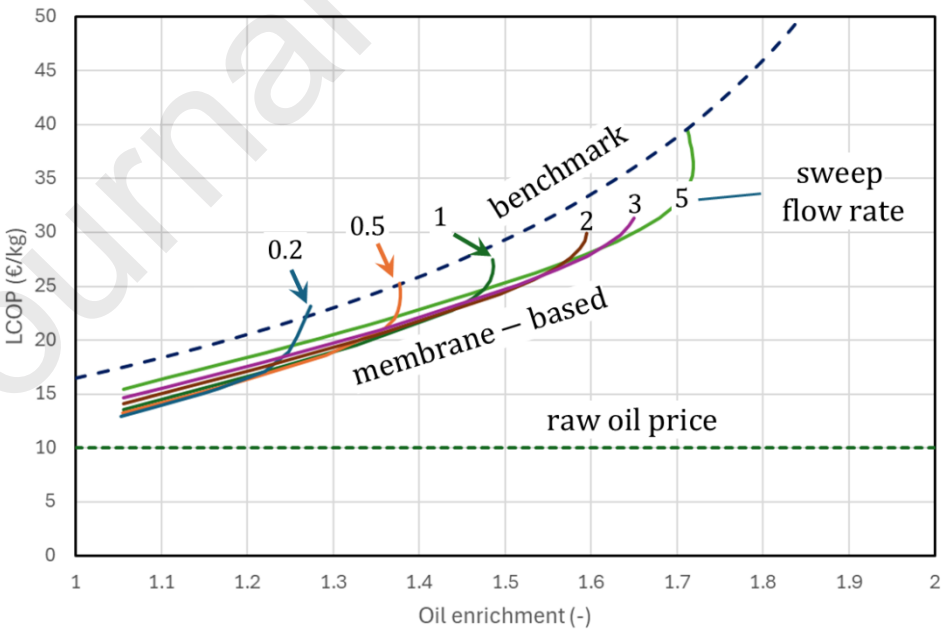

Figure 13: LCOP comparison between membrane-based process at different sweep ethanol flow rates (in labels in kmol/h) and benchmark process. Membrane-based process is operated with Δp=50 bar and OE_{id}=1.9.

While comparable from an expenditure point of view, the cases with different sweep ethanol flow rates have different impact in terms of energy consumption and carbon emissions, as reported in Figure 14. On the left

side, the SEC shows that the sweep flow rate should be maintained below 500 mol/h to have lower consumptions compared to benchmark. It should however be considered that this comparison have been obtained assuming an average electricity production efficiency of 45% with an average GWP value. The usage, for example, of renewable energy sources, for which production efficiency is assumed 100% and with lower GWPs, would move the results more in favor of membrane-based process, allowing to use higher sweep flow rate and therefore making it competitive for a broader range of enrichment values.
On the right side, the equivalent carbon dioxide emissions shows that membrane-based case can have lower emissions up to 2 kmol/h of sweep flow rate in all range of enrichment. Compared to energy consumptions, emissions of the benchmark are penalized since they include also raw oil contribution, and benchmark have in general higher oil consumption. A sensitivity analysis has also been performed by considering the footprint of the oil at the two extremes of the range, with a specific emission of 830 g_{CO2}/kg_{oil} and 2,690 g_{CO2}/kg_{oil} respectively. In the first case, benchmark resulted in comparable emissions (2,600 g_{CO2}/kg_{oil}) for an enrichment of 1.47 and a maximum sweep flow rate of 1 kmol/h. In the latter case, membrane-based case results having lower emissions in all range of enrichment investigated. This is due to the higher oil consumption of the benchmark process, which is therefore more penalized in case of oil with higher footprint.

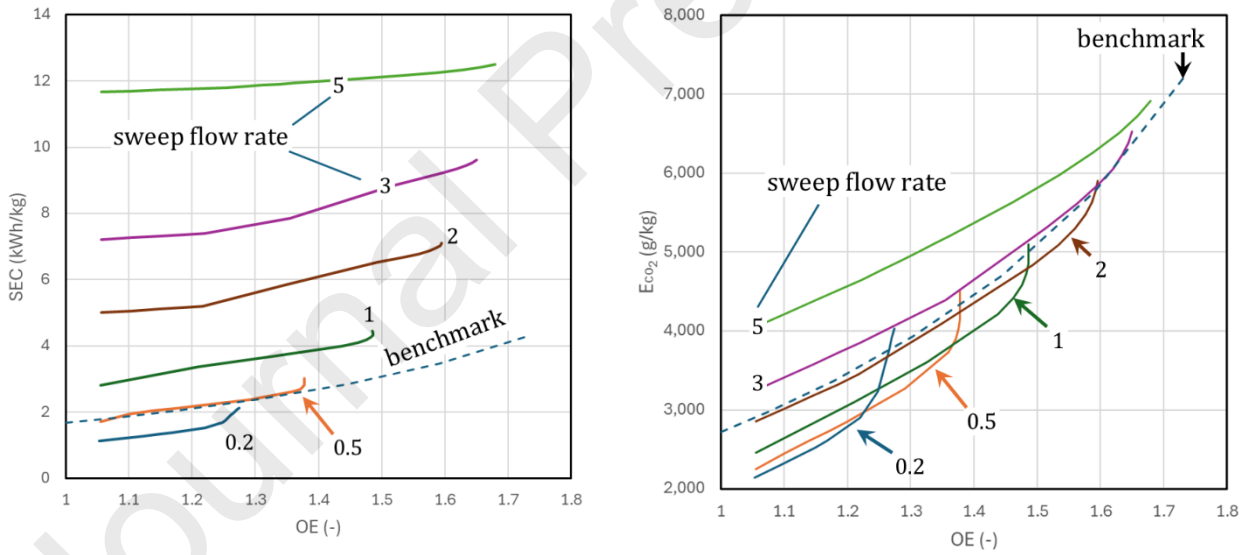

Figure 14: Comparison between energy consumption (SEC) on the left and carbon emissions (E_{CO_2}) on the right for the benchmark and membrane-based processes, the latter at different sweep ethanol flow rates.

5.4 Detailed results for one case study

One case study is selected in order to provide all streams rates and compositions and unit operations consumptions and conditions. The case selected is the one with an oil enrichment of 1.6, corresponding to a final ω3 molar fraction of about 50% (precisely 50.64%). For the benchmark, MD pressure is set at 40 Pa, while MD temperature is regulated to obtain the OE of 1.6, and results 102.3 °C (in Aspen, 136.1 °C). Streams results are reported in Table 10.

Table 10: streams flow rates and compositions for process operating at 40 Pa and MD temperatures 102.3 °C. Names of the streams are referred to Figure 2.

Unit	Raw oil	EtOH	Ethyl esters	In MD	Out MD	glycerol	Enriched oil*
Moles (mol/h)	31.36	69.36	540.548	68.68	31.85	17.48	21.23
Mass (kg/h)	27.64	3.19	51.05	21.23	10.39	1.61	9.3**
T (°C)	25	25	60	54.1	102.3	106.0	114.1
P (bar)	1	1	1	1	1	1	1
			molar fractions				
Glycerol	0.000	0.000	0.042	0.000	0.000	1.000	0.000
Ethanol	0.000	1.000	0.801	0.000	0.000	0.000	0.000
Class 1 TAG	0.109	0.000	0.002	0.000	0.000	0.000	0.006
Class 2 TAG	0.332	0.000	0.005	0.000	0.000	0.000	0.054
Class 3 TAG	0.183	0.000	0.003	0.000	0.000	0.000	0.039
Class 4 TAG	0.236	0.000	0.004	0.000	0.000	0.000	0.081
Class 5 TAG	0.141	0.000	0.002	0.000	0.000	0.000	0.070
Class 1 EE	0.000	0.000	0.014	0.109	0.025	0.000	0.019
Class 2 EE	0.000	0.000	0.042	0.332	0.217	0.000	0.163
Class 3 EE	0.000	0.000	0.023	0.183	0.157	0.000	0.118
Class 4 EE	0.000	0.000	0.030	0.236	0.322	0.000	0.242
Class 5 EE	0.000	0.000	0.018	0.141	0.278	0.000	0.208
NaOH	0.000	0.000	0.014	0.000	0.000	0.000	0.000
Water	0.000	0.000	0.000	0.000	0.000	0.000	0.000
ω3 (mol/h)	29.777	0.000	29.777	29.777	16.113	0.000	16.113

*Enriched oil stream assumes that ethanol and water are fully removed
**mass of enriched product is not results obtained in Aspen, as for the other streams, but its calculated starting from molar flow of acids in the stream (31.865 mol/h), dividing by 3 (to have equivalent TAGs) and assuming a molar mass of 876.115 g/mol.

Operating conditions, energy duties, costs and GHGs emissions for the different units of the process are reported in Table 11.

Table 11: power duties, costs and emissions of the unit operations for the case study in Table 10. Distillation columns have both values at the reboiler (R) and at the condenser (C)

Unit	T (°C)	p (bar)	Th. Power (kW)	El. Power (kW)	Utility (El + Th) cost (k€/y)	Component cost (k€)
Trans. Reactor	60	1	0.16	0	Neglected	50.82
EtOH recovery	168^{R} / 29.1^{C}	0.1	8.4^{R} /-6.6^{C}	3.38	5.758	123.75
Washing column	54.1	1	0	0	0	In others
Salt Reactor	50	1.1	-0.14	0	0	In others
Glycerol recovery	125^{R} / 75.2^{C}	0.4	4.0^{R} /-3.7^{C}	1.6	2.741	35.87
Molecular distillation	102.3	0.0004	4.24	1.7	2.906	89.89
Trans. Reactor 2	60	1	-0.05	0	0	In others
EtOH recovery 2	130.5^{R} / 29.1^{C}	0.1	0.57^{R} / -0.2^{C}	0.228	390	57.85
Others (mixers, pumps, all remaining)	/	/	0	0	0	50
Total	/	/	17.21	6.88	11.793	408.2

For the membrane case, OE of 1.6 can be obtained for different conditions: the ones selected are for a transmembrane pressure of 50 bar, a composition at the membrane inlet relative to an enzymatic enrichment

of OE_{id}=1.9 and a sweep flow rate of 3 kmol/h. Indeed, among the different sweep flow rates, 3 kmol/h guarantees the lower LCOP at OE=1.6 (as in Figure 13) and has comparable emissions with the benchmark (as in right side of Figure 14). Stream results are listed in Table 12, while unit operation conditions in Table 13. In these conditions, membrane area to obtain an OE=1.6 is 0.3 m^2.

Table 12: streams flow rates and compositions for the membrane-based process. Names of the streams are referred to Figure 4.

Unit	Raw oil	EtOH	Esterified oil	EtOH sweep	Retentate	Permeate	Enriched oil*
Moles (mol/h)	25.213	15.485	651.676	3,000	547.578	3,104.1	23.653
Mass (kg/h)	22.091	0.712	42.722	96.127	27.094	111.754	9.3**
T (°C)	25	25	40	40	40	40	45.65
P (bar)	1	1	1	1	51	1	51
			molar fractions				
Ethanol (including glycerol)	0.000	1.000	0.9000	1.000	0.9568	0.9866	0.0000
TAG	1.000	0.000	0.0025	0.000	0.0020	$1.81 \cdot 10^{-4}$	0.0451
DAG	0.000	0.000	0.0111	0.000	0.0111	$3.72 \cdot 10^{-4}$	0.2562
MAG	0.000	0.000	0.0172	0.000	0.0186	$3.46 \cdot 10^{-4}$	0.4294
EE	0.000	0.000	0.0692	0.000	0.0116	$1.25 \cdot 10^{-2}$	0.2693
ω3 (mol/h)	23.94	0	23.94	0	16.085	7.855	16.085

*Enriched oil stream assumes that ethanol and water are fully removed

**mass of enriched product is not results obtained in Aspen, as for the other streams, but its calculated starting from molar flow of acids in the stream (31.865 mol/h), dividing by 3 (to have equivalent TAGs) and assuming a molar mass of 876.115 g/mol.

Table 13: power duties, costs and emissions of the unit operations for the membrane case. Distillation columns have both values at the reboiler (R) and the condenser (C)

Unit	T (°C)	p (bar)	Th. Power (kW)	El. Power (kW)	Utility (El + Th) cost (k€/y)	Component cost (k€)
Trans. Reactor	40	1	0	0	Neglected	54.6
Polymeric membrane	40	50	0	0	Neglected	1.22
EtOH recovery RET (reboiler conditions)	45.7^R / 15.4^C	0.1	5.66^R / -7.1^C	2.26	3.880	106.1
EtOH recovery PER (reboiler conditions)	170^R / 15.5^C	0.4	39.8^R /-40.97^C	15.92	27.248	266.6
Others (mixers, pumps, all remaining)	/	/	0	0	0	50
Total	/	/	45.46	18.184	31.128	478.6

The KPIs, compared for the two processes, are reported in Table 14.

Table 14: KPIs for the case study analyzed.

Parameter	units	benchmark	membrane
Enriched oil production	kg/h	9.3	9.3
Enriched oil production*	L/h	10	10
Technical KPIs			
Oil enrichment	-	1.6	1.6
Target recovery	-	0.545	0.672

Environmental KPIs			
Specific Energy Consumption	kWh/kg	3.47	12.3
GHG specific production	g_{CO2eq}/kg	5,772.1	5,849.7
Economic KPI			
LCOP	€/kg	33.14	27.84

*Calculated from molar flow assuming an average molar volume of 0.9421 L/mol

With the costs compositions reported in Figure 15.

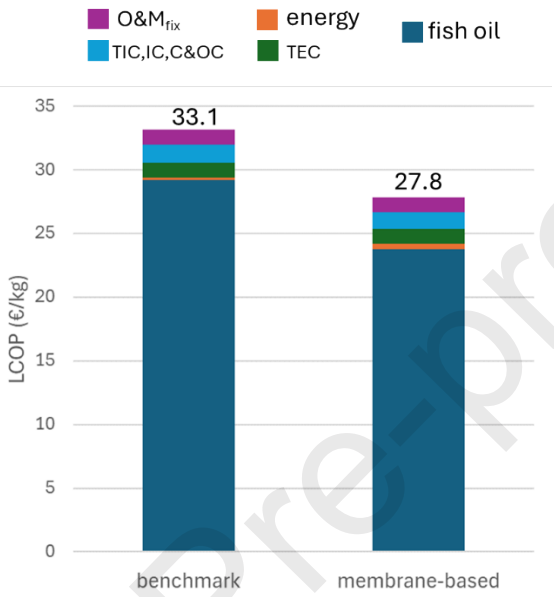

Figure 15: LCOP costs structure for benchmark and membrane-based case, when OE=1.6.

6. Conclusions

In this article, a techno-economic comparison allowed to assess the performance of a membrane-based process to enrich ω3 in fish oil against what can be obtained by a conventional process, which uses a non-selective transesterification reactor and a molecular distillation section to separate the esters. Since there is not a specific target on the oil enrichment, the analyses were performed in all the range of enrichments achievable in both processes.

For the benchmark process, MD temperature is the operating variable that influences the oil enrichment. In general, a more enriched oil represents a more valuable product, but it also has a higher production cost due to the higher oil input necessary to produce it. Based on a validated modelling approach on MD, a curve *ω3 saved* (TR) *vs oil enrichment* (OE) is provided that describes the plant technical performance.

In the membrane-based process, short-chain fatty acids are selectively detached in the enzymatic reactor, and a polymeric membrane removes preferentially the EE fraction of the oil. A model of the reactor is developed, based on a kinetic model developed in another article, as well as a 1D model of the membrane, based on permeability values derived from ad-hoc experimental tests. In this layout, the reactor and the membrane are studied separately, describing the influence of ethanol fraction and enzyme loading in the reactor and of membrane area, sweep ethanol flow rate, transmembrane pressure in the membrane. The

coupling between reactor and membrane is also studied, by selecting as case study a glyceride fraction ideal enrichment in the reactor of a factor 1.9. Transmembrane pressure has been set to 50 bar, to always guarantee a positive flux of ethanol. Ethanol sweep flow rate should be tuned based also on process considerations, due to high energy consumptions for the distillation column and related emissions.

From technical point of view, membrane-based solutions (with sweep flow rate from 0.2 to 5 kmol/h) outperform the benchmark in terms of oil consumption while requires a higher energy consumption, mainly due to the necessity to treat a high sweep flow of ethanol to improve membrane performance. In the economic comparison, membrane-based process turned out to be convenient in all its enrichment range, up to OE=1.7, corresponding to an ω3 molar fraction of 53.81%. From carbon emissions point of view, the membrane-based case can be convenient if sweep flow rate is limited up to 2 kmol/h.

At 1.6, a detailed comparison is made between benchmark and membrane-based case with 3 kmol/h as sweep flow. LCOP results 33.14 €/kg for the benchmark and 27.8 using membranes, and while energy consumption is 3.5 times higher for the membrane-based case (12.3 vs 3.47 kWh/kg), related equivalent CO_2 emissions are comparable (5,849.7 vs 5,722.1 g_{co2eq}/kg), due to higher target recovery using membranes (67.2% vs 54.5%) and then higher emissions related to raw oil used in benchmark process.

In conclusion, this article assesses the potentialities of the usage of polymeric membranes in oil enrichment plants, based on a detailed models of the unit operations and of the overall plants for ω3 concentration. Compared to other works in literature [28], where the product was a highly-enriched oil with very high capital costs [40], membrane-based solution shows convenience when ω3 concentrations requirements are modest, such as where ω3 represent about 55% of the acids of the enriched product. As an outlook, membranes material must be studied to optimize separation selectivity and permeability, then reducing requirements in terms of sweep flow rate and the associated energy duty, while also reducing the necessary oil input.

CRediT authorship contribution statement

Michele Ongis: Conceptualization, Validation, Investigation, Writing – original draft. **Gioele Di Marcoberardino**: Investigation, Writing – review and editing. **Dominic Ormerod**: Experimental analysis. **Fausto Gallucci**: Supervision, Writing – review and editing. **Marco Binotti**: Conceptualization, Validation, Investigation, Writing –review and editing.

Declaration of competing interests

The authors declare that they have no known competing financial interests or personal relationships that could have appeared to influence the work reported in this paper.

Acknowledgments

This project has received funding from the European Union's Horizon 2020 Research and Innovation Program under grant agreement No. 869896 (MACBETH).

Nomenclature

OE	Oil enrichment [-]
TR	Target recovery [-]
$\dot{n}$	Molar flow [mol/s]
x	Molar fraction [-]
SEC	Specific energy consumption [-]
$\dot{W}$	Total inlet electric power [kW]
$\dot{Q}$	Total inlet thermal power [kW]
$\dot{m}$	Mass flow [kg/s]
$E_{CO_2,eq}$	Emissions of CO_2 equivalent [g_{co2}/kg]
GWP_{el}	Global warming potential of electricity production [g_{co2}/kWh]
GWP_{th}	Global warming potential of thermal energy production [g_{co2}/kWh]
$LCOP$	Levelized cost of product [€/kg]
TPC	Total Plant Cost [€]
CCF	Carrying Charge Fraction [1/y]
$O\&M_{fix}$	Operation and Maintenance fixed costs [€/y]
$O\&M_{var}$	Operation and Maintenance variable costs [€/y]
h_{eq}	Equivalent hours of yearly operations [h/y]
TEC	Total equipment cost [€]
$\%TIC$	Share of installation costs [-]
$\%IC$	Share of indirect costs [-]
$\%C\&OC$	Share of contingencies costs [-]
C_k	Cost of equipment component k [€]
C_k^0	Cost of equipment component k at reference size [€]
S_k	Size of the equipment component k [kg/h or kg/s or m^2]
S_k^0	Reference size of the equipment component k [kg/h or kg/s or m^2]
n	Exponent in the size scale factor [-]
$CEPCI_y$	Chemical Engineering Plant Cost Index at year y [-]
rr	Reaction rate [mol/(h·g)]
n	Moles [mol]
t	Time [h]
m	Mass [g]
k	Reaction rate specific for unitary enzyme beads loading [(50 mL_{sol})/(mM·h·g_{beads})]
a	Coefficient in the exponent for the mathematical fitting expression of ϑ
P	Probability of detachment [-]
N	Number of total types of fatty acids detected [-]
j	Permeation flux [mol/(m^2·h)]
$\wp$	Permeability [mol/(m^2·h)]
R	Universal gas constant [J/(mol·K)]
T	Temperature [K]
v_{mol}	Molar volume [m^3/mol]
A	Membrane area
ΔP	Transmembrane pressure (i.e. retentate pressure – permeate pressure) [bar]
Greek symbols	
$\eta_{el,ref}$	Average electricity production efficiency [-]
ϑ	Reaction rate per unit concentrations of the reactants [s/(mol·g)]
ψ_{DAG}^{TAG}	Boolean variable to state if a specific DAG can be obtained by a specific TAG

Journal Pre-proofs

ψ_{MAG}^{DAG}	Boolean variable to state if a specific MAG can be obtained by a specific DAG
δ	Higher glyceride in the UD to obtain the lower glyceride z
Subscripts	
EPA	Relative to EPA
DHA	Relative to DHA
$all\ acids$	Relative to the sum of all acids
$enriched\ oil$	Relative to the enriched oil (product)
$raw\ oil$	Relative to the raw fish oil (feedstock)
i	Relative to a specific fatty acid i
gly	Relative to glycerol
$EtOH$	Relative to ethanol
$R.1$	Relative to reaction R.1
$R.2$	Relative to reaction R.2
$R.3$	Relative to reaction R.3
$enzy$	Relative to the enzyme beads
k	Relative to a specific ester form in the simple model ($k = TG, DG, MG, EE$)
f	Relative to the forward reaction
b	Relative to the backward reaction
z	Relative to a generic component
j	Acid that should be detached from component δ to make z
q	In the kinetic models, relative to ethanol volumetric fraction q
y	Reference year or generic component in permeation model
ret	Relative to the retentate (and feed) side of the membrane
per	Relative to the permeate side of the membrane
$sweep$	Relative to the ethanol sweep flow
Superscripts	
EE	Relative to fatty acids in ethyl ester form
TAG	Relative to fatty acids in triglyceride form
DAG	Relative to fatty acids in diglyceride form
MAG	Relative to fatty acids in monoglyceride form
k	Relative to a specific ester form in the simple model ($k = TG, DG, MG, EE$)
Abbreviations	
PUFA	Polyunsaturated fatty acids
TAG	Triglyceride
EPA	Eicosapentaenoic acid
DHA	Docosahexaenoic acid
EE	Ethyl ester
ME	Methyl ester
FFA	Free fatty acid
KPI	Key performance indicator
GC-FID	Gas chromatography – Flame ionization detector
FAME	Fatty acid methyl ester
SSR	Sum of the squared residuals
SST	Total sum of squares
DAG	Diglyceride
MAG	Monoglyceride
OE	Oil enrichment
TR	Target recovery
ODE	Ordinary differential equation

Journal Pre-proofs

Appendix A. Additional materials

Table 15: parameters for the reaction rate calculations of 5 main fatty acids [26]. Parameters *k* are tabulated in grams of enzyme beads for 50 mL of oil-ethanol solution.

Fitted acid	$k_{i,f}$	$k_{i,b}$	$a_{i,f}$	$a_{i,b}$
(-)	$\left(\frac{50\ \mathrm{mL_{sol}}}{\mathrm{mM}\cdot\mathrm{h}\cdot\mathrm{g_{beads}}}\right)$	$\left(\frac{50\ \mathrm{mL_{sol}}}{\mathrm{mM}\cdot\mathrm{h}\cdot\mathrm{g_{beads}}}\right)$	$(-)$	$(-)$
C16:0	0.00058	0.000133	30.66	92.19
C16:1	0.00013	0	28.60	0
C18:1 cis11	0.00024	0.000028	28.58	38.13
C20:5 (EPA)	0.00005	0	29.31	0
C22:6 (DHA)	0.00002	0	21.38	0

For the other 8 acids, $\vartheta_{i,f}$ and $\vartheta_{i,b}$ are calculated from the relations in Table 16.

Table 16: reaction rates for the other acids [26]

Acid name	Acid code	Modelled ϑ_i
(-)	(-)	(-)
Myristic	C14:0	$\vartheta_{C14:0} = 0.95 \cdot \vartheta_{C16:0}$
Stearic	C18:0	$\vartheta_{C18:0} = \vartheta_{C16:0}$
Oleic	C18:1 cis9	$\vartheta_{C18:1\ cis9} = 1.08 \cdot \vartheta_{C16:1}$
Linoleic	C18:2	$\vartheta_{C18:2} = \vartheta_{C16:1}$
Linolenic	C18:3	$\vartheta_{C18:3} = \vartheta_{C16:1}$
Arachidic	C20:0	$\vartheta_{C20:0} = 1.2 \cdot \vartheta_{C22:6}$
Eicosenoic	C20:1	$\vartheta_{C20:1} = \vartheta_{C18:1\ cis11}$
DPA	C22:5	$\vartheta_{C22:5} = \vartheta_{C20:5}$

Appendix B. Derivation of flux expression

Fundamental statement is that flux $\dot{J}_i$ of component i is proportional to a gradient in chemical potential μ_i along spatial direction x

$$\dot{J}_i = -K_i \cdot \frac{d\mu_i}{dx}$$

and it is assumed that the driving force is reduced to concentration and pressure gradients.

$$\frac{d\mu_i}{dx} = R \cdot T \cdot dln(\gamma_i \cdot c_i) + v_i \cdot dp$$

Solution-diffusion model assumes that the intramembrane pressure is uniform as in the high-pressure side, and therefore the chemical potential gradients is only due to a concentration gradient.
Under this assumption, it results

$$\dot{J}_i = -K_i \cdot R \cdot T \cdot dln(\gamma_i \cdot c_i)$$

and calculating the derivative and assuming the activity coefficient γ_i constant in x it becomes

$$\dot{J}_i = -K_i \cdot R \cdot T \cdot \frac{1}{\gamma_i \cdot c_i} \cdot \gamma_i \cdot \frac{dc_i}{dx}$$

and by defining diffusivity $D_i = R \cdot T \cdot K_i / c_i$

$$\dot{J}_i = -D_i \cdot \frac{dc_i}{dx}$$

that is the well-known Fick's law, which can be integrated over the membrane thickness leading to

$$\dot{J}_i = D_i \cdot \frac{c_{i,0,m} - c_{i,\delta,m}}{\delta}$$

where δ is the membrane thickness.
From this expression, the form of the transport equation depends on how concentrations are related to process parameters, that depends in turn on the phase (gas or liquid) and on the equilibrium conditions with the membrane surface and the transport mechanism.

In nanofiltration process investigated in this article, the model is derived from the observation that at the permeate liquid-membrane interface it is assumed to exist a jump of the pressure from high value to low value, while it is assumed that bulk liquid and liquid in the membrane are at equilibrium, and therefore they have the same chemical potential $\mu_{i,\delta} = \mu_{i,\delta,m}$. Then

$$\mu_i^0 + R \cdot T \cdot \ln(\gamma_{i,\delta} \cdot c_{i,\delta}) + v_i \cdot (p_\delta - p_{i,sat}) = \mu_i^0 + R \cdot T \cdot \ln(\gamma_{i,\delta,m} \cdot c_{i,\delta,m}) + v_i \cdot (p_0 - p_{i,sat})$$

and therefore

$$\ln(\gamma_{i,\delta} \cdot c_{i,\delta}) = \ln(\gamma_{i,\delta,m} \cdot c_{i,\delta,m}) + v_i \cdot \frac{(p_0 - p_\delta)}{R \cdot T}$$

Rearranging and assuming a unitary ratio of activity coefficients:

$$c_{i,\delta,m} = c_{i,\delta} \cdot \exp\left(-\frac{v_i \cdot (p_0 - p_\delta)}{R \cdot T}\right)$$

and, by substituting this expression in Fick's law expression (1.6):

$$\dot{J}_i = \frac{D_i}{\delta} \cdot \left[c_{i,0} - c_{i,\delta} \cdot \exp\left(-\frac{v_i \cdot (p_0 - p_\delta)}{R \cdot T}\right)\right]$$

Expression (1.18), converted in molar fraction terms instead of in concentration terms, is the one that will be used in nanofiltration modelling. At the feed side, since pressure is assumed the same outside and inside the membrane, it simply became $c_{i,0,m} = c_{i,0}$.

Journal Pre-proofs

References

[1] W. Deng, Z. Yi, E. Yin, R. Lu, H. You, and X. Yuan, "Effect of omega-3 polyunsaturated fatty acids supplementation for patients with osteoarthritis: a meta-analysis," *J. Orthop. Surg. Res.*, vol. 18, no. 1, pp. 1–11, 2023, doi: 10.1186/s13018-023-03855-w.

[2] H. Zhang *et al.*, "Association between intake of the n-3 polyunsaturated fatty acid docosahexaenoic acid (n-3 PUFA DHA) and reduced risk of ovarian cancer: A systematic Mendelian Randomization study," *Clin. Nutr.*, vol. 42, no. 8, pp. 1379–1388, 2023, doi: 10.1016/j.clnu.2023.06.028.

[3] M. Khorshidi *et al.*, "Effect of omega-3 supplementation on lipid profile in children and adolescents: a systematic review and meta-analysis of randomized clinical trials," *Nutr. J.*, vol. 22, no. 1, pp. 1–11, 2023, doi: 10.1186/s12937-022-00826-5.

[4] I. M. Dighriri *et al.*, "Effects of Omega-3 Polyunsaturated Fatty Acids on Brain Functions: A Systematic Review," *Cureus*, vol. 9, no. 1, pp. 1–11, 2023, doi: 10.7759/cureus.30091.

[5] FAO, *Fats and fatty acids in human nutrition. Proceedings of the Joint FAO/WHO Expert Consultation.*, vol. 55, no. 1–3. 2009. doi: 10.1159/000228993.

[6] D. Xie, Y. Chen, J. Yu, Z. Yang, X. Wang, and X. Wang, "Progress in enrichment of n-3 polyunsaturated fatty acid: a review," *Crit. Rev. Food Sci. Nutr.*, vol. 63, no. 32, pp. 11310–11326, 2022, doi: 10.1080/10408398.2022.2086852.

[7] P. Lembke, "Omega-6/3 fatty acids: Functions, sustainability strategies and perspectives," *Omega-6/3 Fat. Acids Funct. Sustain. Strateg. Perspect.*, pp. 1–427, 2013, doi: 10.1007/978-1-62703-215-5.

[8] I. Eyskens, A. Buekenhoudt, F. Nahra, and D. Ormerod, "Fractionation of fatty acid alkyl ester mixtures and opportunities for large-scale separation," *Trends Chem. Eng.*, vol. 18, pp. 77–113, 2020.

[9] P. Rossi *et al.*, "FRACTIONATION AND CONCENTRATION OF OMEGA-3 BY MOLECULAR DISTILLATION," in *Eicosapentaenoic Acid: Sources, Health Effects and Role in Disease Prevention*, N. Gotsiridze-Columbus, Ed. Nova Science Publishers, Inc., 2007, pp. 1–27.

[10] J. Dyerberg, P. Madsen, J. M. Møller, I. Aardestrup, and E. B. Schmidt, "Bioavailability of marine n-3 fatty acid formulations," *Prostaglandins Leukot. Essent. Fat. Acids*, vol. 83, no. 3, pp. 137–141, 2010, doi: 10.1016/j.plefa.2010.06.007.

[11] S. Ghasemian, M. A. Sahari, M. Barzegar, and H. A. Gavlighi, "Concentration of Omega-3 polyunsaturated fatty acids by polymeric membrane," *Int. J. Food Sci. Technol.*, vol. 50, no. 11, pp. 2411–2418, 2015, doi: 10.1111/ijfs.12907.

[12] Macbeth Consortium, "MACBETH project," 2019. https://www.macbeth-project.eu/

[13] P. Marchetti, M. F. Jimenez Solomon, G. Szekely, and A. G. Livingston, "Molecular separation with organic solvent nanofiltration: A critical review," *Chem. Rev.*, vol. 114, no. 21, pp. 10735–10806, 2014, doi: 10.1021/cr500006j.

[14] P. Marchetti and A. G. Livingston, "Predictive membrane transport models for Organic Solvent Nanofiltration: How complex do we need to be?," *J. Memb. Sci.*, vol. 476, pp. 530–553, 2015, doi: 10.1016/j.memsci.2014.10.030.

[15] N. F. Ghazali and K. M. Lim, "Mass Transport Models in Organic Solvent Nanofiltration: A Review," *J. Adv. Res. Fluid Mech. Therm. Sci.*, vol. 76, no. 3, pp. 126–138, 2020, doi: 10.37934/arfmts.76.3.126138.

[16] V. H. Hegde, M. F. Doherty, and T. M. Squires, "the Classical Models of Membrane Transport," *Science (80-.).*, vol. 191, no. July, pp. 186–191, 2022.

[17] J. G. Wijmans and R. W. Baker, "The solution-diffusion model: a review," *J. Memb. Sci.*, vol. 107, pp. 1–21, 1995, doi: 10.1016/S0166-4115(08)60038-2.

[18] B. Shi, D. Peshev, P. Marchetti, S. Zhang, and A. G. Livingston, "Multi-scale modelling of OSN batch concentration with spiral-wound membrane modules using OSN Designer," *Chem. Eng. Res. Des.*, vol. 109, pp. 385–396, 2016, doi: 10.1016/j.cherd.2016.02.005.

[19] P. Silva, L. G. Peeva, and A. G. Livingston, "Organic solvent nanofiltration (OSN) with spiral-wound membrane elements-Highly rejected solute system," *J. Memb. Sci.*, vol. 349, no. 1–2, pp. 167–174, 2010, doi: 10.1016/j.memsci.2009.11.038.

[20] P. Silva and A. G. Livingston, "Effect of solute concentration and mass transfer limitations on transport in organic solvent nanofiltration - partially rejected solute," *J. Memb. Sci.*, vol. 280, no. 1–2, pp. 889–898, 2006, doi: 10.1016/j.memsci.2006.03.008.

[21] N. Stafie, D. F. Stamatialis, and M. Wessling, "Insight into the transport of hexane-solute systems through tailor-made composite membranes," *J. Memb. Sci.*, vol. 228, no. 1, pp. 103–116, 2004, doi: 10.1016/j.memsci.2003.10.002.

[22] L. S. White, "Transport properties of a polyimide solvent resistant nanofiltration membrane," *J. Memb. Sci.*, vol. 205, no. 1–2, pp. 191–202, 2002, doi: 10.1016/S0376-7388(02)00115-1.

[23] L. G. Peeva, E. Gibbins, S. S. Luthra, L. S. White, R. P. Stateva, and A. G. Livingston, "Effect of concentration polarisation and osmotic pressure on flux in organic solvent nanofiltration," *J. Memb. Sci.*, vol. 236, no. 1–2, pp. 121–136, 2004, doi: 10.1016/j.memsci.2004.03.004.

[24] D. Peshev and A. G. Livingston, "OSN Designer, a tool for predicting organic solvent nanofiltration technology performance using Aspen One, MATLAB and CAPE OPEN," *Chem. Eng. Sci.*, vol. 104, pp. 975–987, 2013, doi: 10.1016/j.ces.2013.10.033.

[25] Z. Kovács, *Constant-Volume Diafiltration*, vol. Di. 2016. doi: 10.1007/978-3-642-40872-4.

[26] M. Ongis, D. Liese, G. Di Marcoberardino, F. Gallucci, and M. Binotti, "Modelling of enzymatic transesterification for omega-3 fatty acids enrichment in fish oil," *Food Chem.*, p. 141379, 2024, doi: 10.1016/j.foodchem.2024.141379.

[27] M. Ongis, G. Di Marcoberardino, G. Manzolini, F. Gallucci, and M. Binotti, "Membrane reactors for green hydrogen production from biogas and biomethane: A techno-economic assessment," *Int. J. Hydrogen Energy*, vol. 48, no. 51, pp. 19580–19595, 2023, doi: 10.1016/j.ijhydene.2023.01.310.

[28] L. Fiori, M. Volpe, M. Lucian, A. Anesi, M. Manfrini, and G. Guella, "From Fish Waste to Omega-3 Concentrates in a Biorefinery Concept," *Waste and Biomass Valorization*, vol. 8, no. 8, pp. 2609–2620, 2017, doi: 10.1007/s12649-017-9893-1.

[29] IFFO, "measuring footprint of oils." https://www.iffo.com/measuring-footprint-oils (accessed Oct. 08, 2024).

[30] B. L. Mckuin *et al.*, "Comparative life cycle assessment of heterotrophic microalgae Schizochytrium and fish oil in sustainable aquaculture feeds," *Elem. Sci. antropocene*, vol. 2037, pp. 1–22, 2025, doi: https://doi.org/10.1525/elementa.2021.00098.

[31] W. M. Vatavuk, "Updating the Cost Index," *Chemical Engineering*, no. January, pp. 62–70, 2002. [Online]. Available: https://www.chemengonline.com/Assets/File/CEPCI_2002.pdf

[32] "CEPCI index." https://toweringskills.com/financial-analysis/cost-indices/ (accessed Aug. 25, 2024).

[33] G. Di Marcoberardino, S. Foresti, M. Binotti, and G. Manzolini, "Potentiality of a biogas membrane reformer for decentralized hydrogen production," *Chem. Eng. Process. - Process Intensif.*, vol. 129, pp. 131–141, Jul. 2018, doi: 10.1016/J.CEP.2018.04.023.

[34] "Fish Oil Price." https://www.tridge.com/intelligences/fish-oil/price

[35] C. Kick, A. Kline, H. Hladky, and B. Aller, "Using AspenPlus Resources to Model Biodiesel Production Applicable for a Senior Capstone Design Project," *ASEE North-Central Sect. Conf.*, 2013, [Online]. Available: http://people.cst.cmich.edu/yelam1k/asee/proceedings/2013/papers/51.pdf

[36] E. S. Mallmann, C. B. B. Costa, M. R. W. Maciel, and R. M. Filho, *Development of a Computational Tool for Simulating Falling Film Molecular Design*, vol. 26, no. Md. Elsevier B.V., 2009. doi: 10.1016/S1570-7946(09)70124-5.

[37] P. C. Rossi, M. del C. Pramparo, M. C. Gaich, N. R. Grosso, and V. Nepote, "Optimization of molecular distillation to concentrate ethyl esters of eicosapentaenoic (20:5 ω-3) and docosahexaenoic

acids (22:6 ω-3) using simplified phenomenological modeling," *J. Sci. Food Agric.*, vol. 91, no. 8, pp. 1452–1458, 2011, doi: 10.1002/jsfa.4332.

[38] D. R. Woods, *Appendix D: Capital Cost Guidelines*. 2007. doi: 10.1002/9783527611119.app4.

[39] "Borsig Membranes." https://www.osn-membranes.com/what-is-osn/borsig-membranes (accessed Aug. 25, 2024).

[40] L. Fiori, M. Manfrini, and D. Castello, "Supercritical CO2 fractionation of omega-3 lipids from fish by-products: Plant and process design, modeling, economic feasibility," *Food Bioprod. Process.*, vol. 92, no. 2, pp. 120–132, 2014, doi: 10.1016/j.fbp.2014.01.001.

Journal Pre-proofs

- Techno-economic assessment of processes for ω3 fatty acids enrichment in fish oil
- Benchmark process is transesterification followed by molecular distillation
- Innovative route coupling enzymatic reaction and permeation in polymeric membranes
- Performance compared in all range of enrichment values
- Membrane-based process turned out to lower production costs up to 54% concentration

Journal Pre-proofs

CRediT authorship contribution statement

Michele Ongis: Conceptualization, Validation, Investigation, Writing – original draft. **Gioele Di Marcoberardino**: Investigation, Writing – review and editing. **Dominic Ormerod**: Experimental analysis. **Fausto Gallucci**: Supervision, Writing – review and editing. **Marco Binotti**: Conceptualization, Validation, Investigation, Writing –review and editing.

Journal Pre-proofs

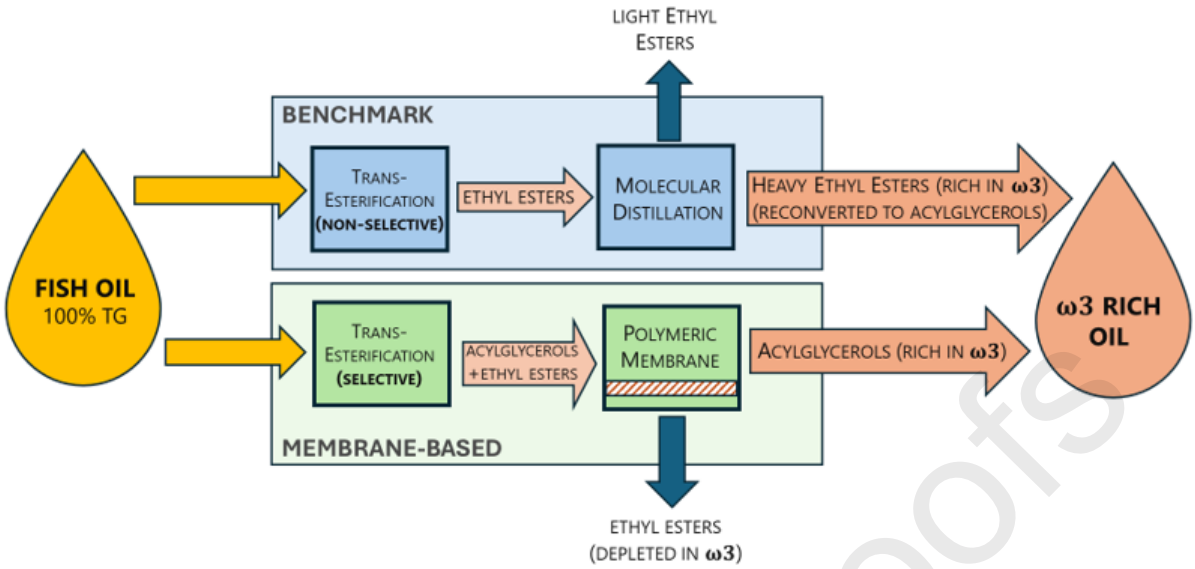

Journal Pre-proofs

Declaration of interests

☒ The authors declare that they have no known competing financial interests or personal relationships that could have appeared to influence the work reported in this paper.

☐ The author is an Editorial Board Member/Editor-in-Chief/Associate Editor/Guest Editor for *[Journal name]* and was not involved in the editorial review or the decision to publish this article.

☐ The authors declare the following financial interests/personal relationships which may be considered as potential competing interests:

Journal Pre-proofs